



HAL
open science

Decreasing uplift rates and Pleistocene marine terraces settlement in the central lesser Antilles fore-arc (La Desirade Island, 16 degrees N)

Jean-Len Leticee, Jean-Jacques Cornee, Philippe Munch, Jan Fietzke, Melody Philippon, Jean-Frederic Lebrun, Lyvane de Min, Auran Randrianasolo

► To cite this version:

Jean-Len Leticee, Jean-Jacques Cornee, Philippe Munch, Jan Fietzke, Melody Philippon, et al.. Decreasing uplift rates and Pleistocene marine terraces settlement in the central lesser Antilles fore-arc (La Desirade Island, 16 degrees N). *Quaternary International*, 2019, 508, pp.43-59. 10.1016/j.quaint.2018.10.030 . hal-02115445

HAL Id: hal-02115445

<https://hal.science/hal-02115445>

Submitted on 22 Oct 2021

HAL is a multi-disciplinary open access archive for the deposit and dissemination of scientific research documents, whether they are published or not. The documents may come from teaching and research institutions in France or abroad, or from public or private research centers.

L'archive ouverte pluridisciplinaire **HAL**, est destinée au dépôt et à la diffusion de documents scientifiques de niveau recherche, publiés ou non, émanant des établissements d'enseignement et de recherche français ou étrangers, des laboratoires publics ou privés.



Distributed under a Creative Commons Attribution - NonCommercial 4.0 International License

1 **Decreasing uplift rates and Pleistocene marine terraces settlement in the central lesser Antilles**
2 **fore-arc (La Désirade Island, 16°N)**

3 Jean-Len Léticée, ^a Jean-Jacques Cornée, ^{a, b*}, Philippe Münch ^b, Jan Fietzke ^c, Mélodie Philippon ^a, Jean-
4 Frédéric Lebrun ^a, Lyvane De Min ^{a, b}, Auran Randrianasolo ^a

5 ^a *Géosciences Montpellier, Université des Antilles, CNRS, Pointe à Pitre, Guadeloupe, FWI*

6 ^b *Géosciences Montpellier, Université de Montpellier, CNRS, Montpellier, France*

7 ^c *GEOMAR, Helmholtz Centre for Ocean Research, Kiel, Wischhofstr, 1-3, 24148 Kiel Germany*

8 Corresponding author: jean-jacques.cornee@gm.univ-montp2.fr (J.-J. Cornée)

9

10 **Abstract**

11 This study investigates the Lesser Antilles forearc at the latitude of Guadeloupe Archipelago and
12 evidences that La Désirade Island, the eastermost island of the forearc, displays a staircase coastal
13 sequence including four uplifted marine terraces and an upper reefal platform with mean shoreline
14 angle elevations ranging from 10 and 210 m above sea level (asl). The platform paleobathymetry is
15 constraint by a detailed analysis of the sediments. We propose a revised morphostratigraphy for this
16 coastal sequence including 5 paleo-shorelines based on six U/Th dating from aragonitic corals from
17 the three lowest terraces combined with paleobathymetric analysis of the fossil corals present in the
18 upper platform allow. Terrace and upper platform carving of construction periods occurred during
19 Marine Isotopic Stages MIS 5e, MIS 9, and during the intervals MIS 15-17, MIS 19-25 and MIS 31-49
20 (upper coral reef platform). Our results evidence a bulk decreasing uplift rate since early Calabrian to
21 Present-Day, clearly documented since 310 ka (MIS 9) (from 0.14-0.19 to *ca* 0 mm/y). Our data are
22 consistent with first the transient influence of the subducting oceanic Tiburon ridge during Calabrian,
23 then with other parametres of the subduction zone since late Calabrian to Present-Day (dip of the
24 slab, basal erosion of the upper plate, inherited structures...).

1

25 **Keywords:** Pleistocene; Lesser Antilles subduction; La Désirade; coral reef terraces; uplift; Tiburon
26 Ridge.

27 1. Introduction

28 Strain pattern and rates observed in fore-arcs of subduction zones are controlled by subduction
29 dynamics, sediment supply at the trench and structural inheritances affecting the upper plate (Noda,
30 2016). In particular, vertical motions in fore-arcs can result from several mechanisms such as: (i)
31 varying geodynamical subduction regime (compressional or extensional) (Shemenda, 1994;
32 Lallemand, 1999), (ii) basal tectonic erosion of the upper plate or accretionary processes (von Huene
33 and Culotta, 1989; Lallemand, 1995; Clift and Vanucci, 2004), (iii) subduction of downgoing plate
34 asperities (such as seamounts, spreading ridges or fracture zone ridges) (e.g. Collot and Fisher, 1989;
35 Dominguez et al., 1998, 2000), (iv) or strain partitioning during oblique subduction driving positive or
36 negative flower structures along strike-slip faults (Gutscher et al., 1998; von Huene et al., 2003;
37 Barnes and Nicol, 2004). Thus, the study and quantification of the distribution and wavelength of
38 vertical tectonic motions through space and time is key to determine long-term subduction
39 dynamics, but also to assess seismic hazards in subduction zones.

40 Submerged and/emerged sequences of marine terraces are very useful datable paleosea levels
41 markers as they allow for calculating uplift or subsidence rates (e.g. Henry et al., 2014; Pedoja et al.,
42 2011, 2014; Saillard et al., 2009, 2011). Coastal uplift rates since MIS 5e have been found significantly
43 higher in highly coupled subduction zones than in other geodynamic settings (Pedoja et al., 2011;
44 Henry et al., 2014). Moreover, coastal uplift rates in fore-arc settings have been found correlated
45 mainly with the distance to the trench (with decreasing uplift rates landward up to ~300 km), the
46 slab dip and the position along the trench (Henry et al., 2014). The tectonic regime of the subduction
47 margin (erosive vs accretionary) and the overriding plate tectonic regime (compressive vs extensive)
48 appear only gently correlated (Henry et al., 2014; Noda, 2016). Noticeably, the convergence velocity,

49 subduction obliquity, oceanic crust age, interplate friction force and overriding plate velocity do not
50 appear correlated with coastal uplift rates of fore-arcs (Henry et al., 2014).

51 The Lesser Antilles subduction is considered as a weakly coupled accretionary subduction zone where
52 an old oceanic lithosphere slowly subducted (2cm/an) beneath the Caribbean plate and with an
53 accretionary compressional fore-arc basin ((e.g. Von Huene and Scholl, 1991; Clift and Vannucchi,
54 2004; Noda, 2016). This description corresponds well to the southern Lesser Antilles where an
55 uplifted sequence of marine terraces has been extensively studied in the outer fore-arc, in the
56 Barbados Island (e.g. Taylor and Mann, 1991; Schellmann and Radtke, 2004). However many
57 sequences of marine terraces also occur in the central Lesser Antilles fore-arc, i.e. to the North of the
58 Martinique Island, but have been more scarcely studied (Désirade: Battistini et al., 1986; Marie-
59 Galante : Feuillet et al., 2004). North of Martinique, the Lesser Antilles subduction zone has a
60 different tectonic regime from the one at the latitude of the Barbados Island exemplified by a
61 narrowed accretionary prism, an extensional overriding plate tectonic regime (Feuillet et al., 2002;
62 De min et al., 2014), the subduction of sediments deeper into the subduction zone (Bangs et al.,
63 2003) and the subduction of aseismic ridges (Bouysson and Westercamp, 1988). We detail here the
64 quantification of vertical motion in La Désirade Island, i.e. the easternmost island (185 km west of
65 the trench) island of the fore-arc, since ~1.5 Ma. In La Désirade Island, a stair-cased marine terraces
66 sequence has been identified since a long time (Lasserre, 1957; Battistini et al., 1986) and Pliocene–
67 Pleistocene carbonate platform deposits reach 210 m in elevation (Andreïeff et al., 1989; Münch et
68 al., 2013). To reach this goal, we acquired a new sedimentological, geomorphological and
69 radiochronological dataset from uplifted constructed (corals) marine terraces and reefal carbonate
70 platforms. This dataset allows us to calculate mean coastal uplift rates of the fore-arc since ~1.5 Ma
71 and to discuss about the fore-arc tectonic structures responsible for terraces uplift and, at
72 subduction-scale, the mechanical behavior of the subduction interface at 16°N latitude in the
73 Caribbean.

74

75 **2. Geodynamic setting**

76 The Lesser Antilles Arc emplaced at the eastern boundary of the Caribbean Plate as a result of the
77 west-southwestward subduction of North America and South America oceanic lithospheres, at a rate
78 of around 2.0 cm/y (e.g. Deng and Sykes, 1995; Dixon et al., 1998; De Mets et al., 2000; Pindell and
79 Kennan, 2009) (Fig. 1). The NW-SE trending Barracuda and Tiburon ridges are the diffuse plate
80 boundary between North and South American plate (Fig. 1). These features accommodate the slow
81 North and South America plate convergence and consist of oceanic fracture zones reactivated since
82 the Middle Miocene, and the Pleistocene respectively (Patriat et al., 2011; Pichot et al., 2012). At La
83 Désirade latitude, the subduction is orthogonal. The ridges trend oblique to the plate motion vector,
84 thus sweeping the subduction zone from North to South at a rate of 2.0 cm/y. Nowadays, the
85 topographic effect of the Tiburon ridge is observed across the outer fore-arc to the East of La
86 Désirade Island (Figs. 1 and 2) (McCann and Sykes, 1984; Bouysse and Westercamp, 1990; Bangs et
87 al., 2003; De Min et al., 2015). Northwestward of La Désirade, the Lesser Antilles trench curves and
88 extends into the E-W Puerto Rico Trench. Northwardly, increasing subduction obliquity resulting
89 from the trench curvature triggers strain partitioning in the upper plate that induced trench-parallel
90 strike-slip combined with trench-parallel extension in the fore-arc (Bouysse and Westercamp, 1990;
91 Feuillet et al., 2002; 2004; Laurencin et al., 2017; Legendre et al., 2018).

92 In the Guadeloupe archipelago fore-arc extensive tectonics is highlighted by two main E-W trending
93 grabens: the Marie-Galante graben and the La Désirade graben (Fig. 2). The Marie-Galante graben is
94 bounded to the North by the Basse-Terre Island, corresponding to the active volcanic arc, and by the
95 Grande-Terre Island, corresponding to a tectonic high, and to the South, by the Marie Galante Island
96 corresponding to a tectonic high. La Désirade Island is located on top of the hangingwall of the main
97 southern border normal faults of the La Désirade graben. The La Désirade tectonic high extends to

98 the South into the submerged Karukéra spur that is the eastern border of the Marie-Galante basin.
99 The age and characteristics of this extensive tectonics and related fore-arc uplift are debated.
100 Based on the study of a flight of reef terraces, Feuillet et al. (2004) proposed that, since 330 ka, the
101 whole archipelago emerged, underwent a uniform uplift and regional westward tilting by 0.35°.
102 Following these authors, La Désirade, closest island to the trench, should have emerged since 330 ka
103 and then should have been more uplifted than other islands in relation with a westward tilting.
104 Feuillet et al. (2002) interpreted these features as trench-parallel extension linked to slip partitioning
105 along the northern part of the Lesser Antilles subduction zone. Feuillet et al. (2004) suggested that
106 the tilt probably resulted from a transient deformation episode at the subduction interface that
107 predated the late Pleistocene.

108 Based on the study of Pliocene-Pleistocene carbonate platforms, Cornée et al. (2012) and Münch et
109 al. (2013, 2014) evidenced that the emergence of islands of Guadeloupe archipelago occurred in the
110 1.07-1.54 Ma interval, i.e. 0.74 to 1.21 Ma earlier than proposed by Feuillet et al. (2004). Offshore,
111 De Min et al. (2015) showed that the Karukéra spur experienced three main extensional episodes (i.e.
112 Eocene?–Oligocene, Late Miocene and since Calabrian) with alternations between uplift and
113 subsidence periods. The main extensional directions evolved from NW–SE, E–W to N–S, respectively
114 (De Min et al., 2015). Since Calabrian, the Karukéra spur tilted to the east-northeast triggering
115 subsidence of the Eastern Flank (more than 2000 m) and emersion of both the northern part up to La
116 Désirade and the western flank of the spur (De Min et al., 2015).

117

118 **3. Geomorphology and geological setting**

119 La Désirade Island is 11.5 km long, 2 km large and reaches a maximum altitude of 276 m above sea
120 level (asl). The island consists of Jurassic to Cretaceous metamorphic basement capped by *ca* 120 m
121 thick Pliocene-Pleistocene carbonate platform deposits (e.g. Westercamp, 1980; Léticée, 2008;

122 Lardeaux et al., 2013; Münch et al., 2013; 2014). These carbonate platform deposits span the
123 Zanclean–Calabrian interval (Léticée, 2008; Münch et al., 2013, 2014). The youngest deposits of this
124 platform (1.54-1.07 Ma interval; Münch et al., 2014) correspond to a thick-branched *Acropora*
125 *palmata* reef platform reaching a 10 to 15 m thickness at maximum (Fig. 4). These deposits occur
126 near sea-level at Anse des Galets, Beauséjour at the western tip of the island, and at an elevation of
127 210 meters asl at the top of the eastern part of the island. These differences in elevation were
128 triggered by a major episode of extensional tectonics accommodated by both N90°E and N110°E-
129 N130°E normal faults, either during Ionian (Feuillet et al., 2004) or during Early Calabrian (Münch et
130 al., 2014). This episode caused the emergence of Pliocene-Pleistocene carbonate platforms that now
131 form the Upper Plateaus, and their local tilting (Lardeaux et al., 2013; Münch et al., 2014).

132 At La Désirade the amplitude of the tides is less than a meter (30 cm with a maximum from 50 to 60
133 cm) (e.g. BRGM, 2010). The northern coast of La Désirade is dominated by erosion and high and
134 steep cliffs with few preserved raised beaches and coral reef terraces. On the southern coast of the
135 island, sheltered from wind and swells by fringing reefs, uplifted beaches, coral reef terraces and
136 wavecut surfaces are better preserved. There, a coral reef terrace corresponding to the Last
137 Interglacial maximum has been studied and dated (Battistini et al., 1986; Feuillet et al., 2004). In the
138 southwesternmost part of the island, at Pointe Frégule (Fig. 3A), U/Th ages on corals provided $119 \pm$
139 9 ka (Battistini et al., 1986, but ages were provided without U and Th concentrations, $^{234}\text{U}/^{238}\text{U}$
140 values, and $^{230}\text{Th}/^{232}\text{Th}$ values) and 141 ± 7 ka (Feuillet et al., 2004). In the northeastern part, at Baie-
141 Mahault (Fig. 3A), Battistini et al. (1986) provided an age of $272 +72$ to -43 ka.

142 Elsewhere in the Guadeloupe archipelago, Pliocene-Pleistocene carbonates platforms, named Upper
143 Plateaus, are fringed by up to four mid-late Pleistocene coral reef terraces or wavecut surfaces,
144 which were identified at Grande Terre and Marie Galante (de Reynal de Saint Michel, 1966;
145 Westercamp, 1980; Battistini et al., 1986; Feuillet et al., 2004) (Fig. 2). In these islands, the
146 lowermost terrace, at an elevation of 5-10 m asl, was dated from the 158 – 110 ka interval (Last

147 Interglacial Maximum terrace; Battistini et al., 1986; Feuillet et al., 2004). At Marie Galante, a second
148 uplifted marine terrace, occurring at an altitude ranging from 50 to 108 m asl, yielded a model age of
149 249 ka (terrace T2; Villemant and Feuillet, 2003; Feuillet et al, 2004). By correlating measured ages of
150 both marine terraces in Marie Galante with the SPECMAP isotopic curve, Feuillet et al. (2004)
151 proposed an age of 330 ka for the emersion of all islands of the archipelago.

152 We investigated La Désirade Island for datable uplifted marine erosional terraces (wavecut surfaces),
153 marine constructional terraces (coral reef) and depositional terraces (beaches) to analyse Pleistocene
154 vertical tectonic motions of the fore-arc.

155

156 **4. Methods**

157 *4.1. High-resolution mapping*

158 We conducted several field-mapping campaigns at 1/10000 scale, mapping with in detail wavecut
159 surfaces and marine terraces. Elevations and spatial extent of the terraces were determined using
160 field mapping, Garmin GPS and a 5m resolution DEM (Litto-3D Guadeloupe, V1, IGN-SHOM 2013).
161 Cross-sections were built using QGIS software (<http://www.qgis.org>) (Fig. 5). Elevation data are from
162 SHOM and function of the Present-Day mean sea level reference (uncertainty is ± 1 m). Special
163 attention was devoted to the location of fossil strandlines, flat and subhorizontal terraces, beach
164 facies, notches, coral reefs, and shoreline angle (Lajoie, 1986; Pirazzoli et al., 1993; Montaggioni and
165 Braithwaite, 2009; Pedoja et al., 2011; Jara-Muñoz et al., 2015) (Fig. 5D). For the coral reef platform
166 (Upper Plateaus), the preserved faunal content allows an estimation of the paleo-bathymetry before
167 its emergence.

168 *4.2. U/Th Dating*

169 We made sure that the necessary conditions for using U-series ages of corals were met by our
170 samples: (i) few or no evidence of recrystallization, (ii) presence of little or no non-radiogenic ^{230}Th
171 and (iii) initial $^{234}\text{U}/^{238}\text{U}$ value in agreement with modern seawater one (1.141 to 1.155; Delanghe et
172 al., 2002). Corals selected for U/Th datations were first examined in thin-sections in order to select
173 aragonite samples and avoid recrystallization or pore-infilling. We determine their mineralogy and
174 quantify their aragonitic content by X-Ray diffraction at the University of Montpellier (Philips X'Pert
175 PRO MPD diffractometer; PANalytical X'Pert HighScore Plus version 3.0.5 software). Each sample was
176 analyzed during one hour between 5 and 60° Theta, with a 0.033° Theta step. We selected six
177 samples that fulfil conditions and yield more than 95% of aragonite.

178 We carried out radiometric U/Th dating using the „AXIOM“ MC-ICP-MS at IFM-GEOMAR Kiel,
179 Germany. About 60 mg of carbonate powder drilled from each sample were dissolved (HNO_3), and 50
180 μl of a pre-mixed $^{229}\text{Th}/^{233}\text{U}/^{236}\text{U}$ -spike solution (“Mix9”) were added before evaporating the samples
181 on hotplates at 90°C under filtered air. Dried samples were dissolved in 7n HNO_3 and passed through
182 ion chromatographic columns containing 2 ml of EICHRON’s UTEVA® resin. After separation, two
183 fractions (U and Th) were measured separately using the MIC (Multi-Ion-Counting) method described
184 by Fietzke *et al.* (2005). We controlled the analytical quality by analyzing the reference standard (HU
185 1) and two blank samples. Secular-equilibrium standard HU-1 gained the $^{230}\text{Th}/^{234}\text{U} = 0.9989 \pm 0.0014$
186 and $^{234}\text{U}/^{238}\text{U} = 0.9994 \pm 0.0011$ activity ratios (95% confidence). Within the limits of uncertainty both
187 isotope ratios match the reference values of 1. Analytical blanks are provided in Table 1. Being
188 typically about 3-4 orders of magnitude lower than the respective sample amounts analytical blanks
189 were practically insignificant but nevertheless data were blank-corrected. We corrected from the
190 non-radiogenic ^{230}Th incorporated during carbonate formation using the following equation:

$$191 \quad ^{230}\text{Th}_{\text{xs}} = ^{230}\text{Th}_{\text{measured}} - ^{230}\text{Th}_{\text{non-rad}} = ^{230}\text{Th}_{\text{measured}} - (0.7 \pm 0.2) * ^{232}\text{Th}_{\text{measured}}$$

192 Where $^{230}\text{Th}_{\text{xs}}$ represents the excess amount of ^{230}Th produced by the decay of uranium.

193 4.3. Uplift rate determination

194 We assigned a sea-level highstand corresponding to a Marine Isotopic Stage to each dated
195 paleoshoreline. Even if large uncertainties remain in estimating paleo-sea level during Pleistocene,
196 we use the long record of paleo-sea levels from Rohling et al. (2014) because it has been validated
197 from two independent methods: (i) deep-sea temperature changes from oxygen isotopes converted
198 into sea level and (ii) hydraulic control of water exchange through a narrow connection with the
199 open ocean in semi enclosed seas (Red Sea and Mediterranean). We give the paleo-sea levels with a
200 wide error margins for each isotopic stage, graphically calculated from the curve of Rohling et al.
201 (2014). Ages of the different interglacial MIS, even if sometimes debated, are the mean ages
202 provided by these authors. Results do not take into account isostatic correction. We estimate relative
203 vertical uplift between each paleoshoreline on the basis of the difference of elevations corrected
204 from paleo-sea levels of Rohling et al. (2014), and the morphostratigraphic model of Lajoie (1986)
205 and Saillard et al. (2009). This stratigraphic model has the following equation: Uplift rate
206 $interval_{T_n/T_{n+1}} = [(elevation\ of\ shoreline\ angle\ of\ Terrace_n - elevation\ of\ shoreline\ angle\ Terrace_{n+1}) -$
207 $(Sea\ level\ at\ MIS_{Terrace\ n} - Sea\ level\ at\ MIS_{Terrace\ n+1})] / (age\ of\ MIS_{Terrace\ n} - age\ of\ MIS_{Terrace\ n+1})$. This
208 equation allows us to propose apparent uplift rates between the formations of two successive
209 shoreline angles related to marine terraces.

210

211 5. Sedimentary facies, paleo-environments and new U/Th age of reefal units

212 5.1. *Acropora palmata* reef platform (top of Upper Plateaus)

213 The platform was uplifted at maximum to an elevation of 210 m asl and displays in growth position
214 massive coral colonies and locally thick-branched *Acropora palmata* colonies (Fig. 4C) and packstones
215 dominated by bivalves and benthic foraminifers (among which Amphisteginids). The general
216 sedimentological features of this unit are indicative of an inner reefal platform depositional
217 environment at very shallow water (Montaggioni and Braithwaite, 2009). Especially, the Caribbean
218 species *A. palmata* optimally lives between sea level and 5 m bsl (Veron, 2000) (Fig. 4D). Thus, we

219 considered in our calculations that the last unit of the Pliocene-Pleistocene carbonate platform was
220 deposited at ca 5 m below sea level (bsl).

221 5.2 *Depositional marine Terrace 1*

222 Terrace 1 was found in the northeastern part of the island as a 500 m wide subhorizontal erosional
223 relict between Pointe Adrien and Pointe du Grand Abaque. The metamorphic basement and the red
224 algal platform deposits are unconformably overlaid by terrace 1 between 90 and 85 m asl (Fig. 3A
225 and 6A), corresponding to the 90 m asl littoral terrace of Lasserre (1961). Above the basement,
226 locally few dm-thick littoral limestones with pebbles are preserved, sometimes encrusted by red
227 algae (Fig. 6B) or bored by lithophagid molluscs. These pebbles are derived from both the
228 metamorphic basement and the Zanclean red algal carbonate platform. Limestones are packstones
229 with coral and oyster fragments, Amphisteginids, regular echinoids and red algae. Discrete notches
230 are locally preserved, carved into the Zanclean red algal carbonate platform deposits (Figs. 3A and
231 5A), and the shoreline angle is located at 90 ± 1 m asl. These deposits are indicative of a very shallow
232 littoral environment and were erroneously mapped as basal deposits of the Zanclean platform by
233 Westercamp (1980).

234

235 5.3. *Depositional marine Terrace 2*

236 The summit of the deposits of Terrace 2 correspond to foreshore deposits or coral buildups at 76 ± 1
237 m asl. These are only found in the eastern part of the island, along 4 km between Pointe Adrien and
238 Baie Mahault (Figs 3, 5 and 7A), corresponding to the 75 m asl littoral terrace of Lasserre (1961). At
239 Route de la Montagne, a well preserved 5 m thick marine terrace rests directly on the metamorphic
240 basement and its top is at 76 ± 1 m asl (Fig. 3A and 7B to E). From base to top, it contains: loose
241 pebbles, normally graded conglomerates with pebbles originating from the basement and the
242 Zanclean red algal platform, calcareous conglomerates bearing Amphisteginids and bioclastic
243 limestones with low-angle planar bedding are found in the uppermost part. These latter are

244 packstones to grainstones with benthic foraminifers (among which Amphisteginids), red algae,
245 gastropods, bryozoans, corals and echinoids. Some coral fragments are coated with encrusting red
246 algae (rhodoliths). Aragonitic *Diploria* coral colonies from the uppermost part of the deposits (Fig. 7E
247 to G) yielded an age older than 500 ka (Sample DS 10-05; Table 2). Based only on the uranium
248 isotope ratio it is possible to calculate a U/U apparent age of 659 -33 ka, +36 ka assuming an initial
249 $^{234}\text{U}/^{238}\text{U}$ activity ratio of 1.146 (modern sea water).

250 All these deposits are indicative of a reefal to peri-reefal depositional environment in foreshore to
251 uppermost shoreface setting (Tucker and Wright, 1990; Montaggioni and Braithwaite, 2009). They
252 were deposited at the foot of a paleocliff transecting the Zanclean platform and the metamorphic
253 basement. The summit of this depositional terrace, at 76 ± 1 m asl, is considered as a shoreline angle
254 level. These deposits were erroneously mapped as basal deposits of the Zanclean platform
255 (Westercamp, 1980).

256 5.4. *Depositional marine Terrace 3*

257 A subhorizontal wavecut surface is scarcely preserved 36 m asl all around the island (Figs. 3 and 5).
258 This surface corresponds to the 35m asl terrace identified at the eastern tip of the island by Lasserre
259 (1961). This wavecut surface is found transecting either the Zanclean red algal platform at Cap
260 Frégule or the basement at Roche du large (Fig. 8D).

261 At *Pointe Doublé*, a depositional marine terrace was also identified (Lasserre, 1961). This terrace is
262 topped by a flat surface at 36 ± 1 m asl and consists of 2.5 m thick karstified grainstones with planar
263 laminations (Fig. 8C) that yielded rounded fragments of red algae, mollusks, Amphisteginids and few
264 basement clasts. These deposits are considered as deposited in foreshore setting and their summit is
265 interpreted as representing a shoreline angle.

266 At *Cul Foncé*, we evidenced a depositional marine terrace made of conglomerates and limestones
267 and topped by a flat surface culminating at 36 ± 1 m asl surface (Fig. 8A and B). This terrace rest

268 against a cliff in the basement between 28 and 36 m asl above an erosion surface (Fig. 9A). In its
269 lower part, occur conglomerates with cross-trough stratifications and planar bedding (Fig 9C).
270 Pebbles are composed of diverse rocks that originate from both the basement and the Zanclean
271 platform. Above, conglomerates evolve into bioclastic limestones with 3D dunes (Fig. 9B), low-angle
272 parallel laminations (Fig. 9C and E), cross-stratifications (Fig. D) and locally hummocky cross-
273 stratifications. Some broken massive coral colonies can be found (Fig. 9E, F).

274 These sediments were deposited into perireefal high energy depositional environment oscillating
275 between foreshore and upper shoreface setting at the foot of a paleocliff (Fig. 8B). The summit of the
276 foreshore deposits at $36 \text{ m} \pm 1 \text{ asl}$ corresponds to the shoreline angle, and notches in the basement
277 can be found at this elevation. The aragonitic coral sample DS10-40 yielded a U/Th age of $306 \pm 6 \text{ ka}$,
278 (Fig. 9, E and F; Table 2). These deposits were erroneously mapped as Zanclean carbonate platform
279 deposits (Westercamp, 1980).

280 5.5. Coral reef Terrace 4

281 Coral reefs of Terrace 4 are well preserved and were previously identified (Lasserre, 1961; Battistini
282 et al., 1986; Feuillet et al., 2004). This constructed terrace can be followed at an elevation between
283 sea level (distal edge) and + 10 m asl (inner edge). The paleo-shoreline angle of this terrace was
284 patchily reconstructed all around the island based on scattered but abundant exposure at 10 m asl:
285 between Baie Mahault and Le Souffleur (Fig. 4A), Cul Foncé (Fig. 8A), Cap Frégule (Fig. 10), Airport
286 quarry, Pointe Fromager (Fig. 11) and Pointe Mancenillier (Fig. 12F). We detail here only the locations
287 where we were able to perform U/Th datings.

288 At *Baie Mahault* (Fig. 12A) massive to columnar corals, mainly *Montastraea* (Fig. 12A and E)
289 associated with *Diploria* and *Porites*, are cropping out landwards whereas *A. palmata* boundstones
290 and *Strombus* accumulations are abundant seawards (Fig. 12, A, D, E). The summit of the deposits is
291 gently dipping (0.5 to 1°) seawards from 10 m to 4 m asl. At the top of the preserved reef deposits is
292 a tens of cm-thick level displaying thin-branched *Acropora* at 5 m asl (Fig. 12A and B). These corals

293 yielded an age at 133.5 ± 0.84 ka (Sample DS 11-43, Fig.12A to C; Tab. 2). This age is much younger
294 and precise than the one previously published, i.e. $272 +72$ to -43 ka (Battistini et al., 1986), and we
295 considered that our new age as the estimate for Terrace 4. The Terrace T4 corresponds to a fringing
296 reef complex in high-energy shallow-water environments, deposited on a seaward low-angle dipping
297 ramp.

298 *In the southwestern part of the island* the reef complex comprises large colonies of *A. palmata*,
299 *Montastraea* and *Diploria* in growth position and coral rubbles and coarse-grained bioclastic
300 limestone with *Strombus*. This complex gently dips to the West, from 10 m asl at Airport Quarry to
301 sea level at Cap Frégule and Pointe Colibri. We performed U/Th dating at 2.5 m asl at Pointe Frégule
302 (Fig. 10F and G). Two aragonitic coral colonies, *A. palmata* (DS 10-12a) and *Montastraea* sp. (DS10-
303 12b) provided ages, 126.09 ± 0.58 ka and 128.19 ± 0.61 , respectively (Fig. 3 and Table 2). These
304 results are in good agreement with the age we obtained for the Terrace 4 in Baie Mahault and with
305 those previously obtained at Pointe Colibri (Battistini et al., 1986; Feuillet et al., 2004).

306 **6. Discussion**

307 *6.1 Ages used for the uplift rates calculation*

308 Some uncertainties remain concerning the ages of terraces 1 and 2. However, we proposed here
309 estimate based on the U/Th ages of terraces 3 and 4 and the estimated age of the *A. palmata* coral
310 platform. We correlated each terrace with the paleo-sea level curve from Rohling et al. (2014) and
311 one or several Marine Isotopic Stage highstand (Fig. 13).

312 Terrace 4 yielded ages ranging between 126-133 ka, indicating that the 10 m asl paleoshoreline
313 formed during the the Last Interglacial Maximum highstand (MIS 5e) dated at 122 ka. Terrace 3
314 yielded an age of 305.76 ± 5.96 ka, indicating that the shoreline angle at 36 ± 1 m asl formed during
315 the 310 ka MIS 9 highstand. Terrace 2 yielded an age of $659 -33$ ka, $+36$ ka, indicating that the
316 shoreline angle at 76 m may have formed during the MIS 15 high sea level at 620 ka or the during the

317 MIS 17 one at 700 ka. In Grande Terre, the *A. palmata* reef platform deposited during the reverse
318 subchron C2r, in the 1.07-1.54 Ma interval (Münch et al., 2014). This platform deposited
319 synchronously in La Désirade and in Marie Galante (Cornée et al., 2012; Münch et al., 2013, 2014).
320 This interval includes two main highstands: MIS 31 at 1.07 Ma and MIS 47 at 1.48 Ma (Fig. 13).

321 As a consequence, the age of Terrace 1 is bracketed by the estimated ages range for Terrace 2,
322 correlated with MIS 15 or MIS 17 highstands, and the age range of *A. palmata* reef platform (MIS 31-
323 47 interval). Consequently, we considered that Terrace 1 was formed in a time span ranging from the
324 high sea-levels MIS 19 to 25, *i.e.* in the 780 to 970 ka taking into account the youngest age (1.07 Ma)
325 for the *A. palmata* reef platform (Fig. 13). However the incertitude on the age of the Terrace 1 could
326 be much greater taking into account an older age for the *A. palmata* reef platform.

327 *6.2. Pleistocene vertical motions in the northern Lesser Antilles fore-arc*

328 In the Guadeloupe Archipelago, apart from La Désirade, uplifted Pleistocene marine terraces also
329 crop out in Grande Terre and Marie Galante. In Grande Terre, only the Last Interglacial Maximum
330 terrace was recognized at an elevation between 0.5 and 6 m asl and was dated between 149 and 158
331 ka (Battistini et al., 1986; Feuillet et al., 2004) (Fig. 14). In Marie Galante, a flight of four uplifted
332 Pleistocene marine terraces was described but only the lowermost one, at an elevation between 2
333 and 15 m asl, was dated accurately between between 110 and 134 ka (Battistini et al., 1986; Feuillet
334 et al., 2004). A modeled age at 249 ± 8 ka was also proposed for a second terrace on Marie Galante
335 that is the second most elevated at 50–108 m asl (T2 *in* Feuillet et al., 2004). This age was calculated
336 in an open system to account for selective mobilities of U-series isotopes in a partly recrystallized
337 (calcite) coral sample (Villemant and Feuillet, 2003). Uplifts are related to a westward tilting and/or
338 local deformation along normal faults bounding the Marie Galante graben. Local deformations result
339 in a lowering of the terraces elevation towards the center of the graben whereas westward tilting of
340 the Marie Galante Island results in higher uplift in the eastern part of the island. In Marie Galante, an
341 uplift rate was calculated for the Last Interglacial Maximum terrace at 0.08 mm/yr (Feuillet et al.,

342 2004). The same authors also calculated higher uplift rates (0.2 mm/yr) taking into account an age of
343 330 ka for the *A. palmata* reef platform (Upper Plateaus) based on the correlation of both dated
344 terraces with the SPECMAP curve. However, the reverse magnetic polarity of the *A. palmata* reef
345 platform (Münch et al., 2014) contradicts the estimated age used for uplift rate calculations and
346 questions the validity of the modeled age of Villemant and Feuillet (2003) for the second most
347 elevated terrace in Marie Galante. As we found an age of 659 -33 ka, +36 ka for T2 (the second most
348 elevated terrace) and 306 ± 6 ka for T3 in La Désirade, the age of the *A. palmata* reef platform is
349 definitely not 330 ka. Thus, only the mean uplift rate of 0.08 mm/yr for the MIS 5 terrace in Marie
350 Galante can be considered valid.

351 In Saint Martin, only the MIS 5 terrace was described and crops out at ca 12 m asl and, in Puerto Rico,
352 the MIS 5 terrace is between 4.5 and 5.5 m asl (synthesis in Pedoja et al., 2014) (Fig. 1). In the
353 Dominican Republic, the MIS 5e terrace is between 10 and 20 m asl (Diaz de Neira et al., 2015). Thus,
354 the uplift of the MIS 5 terrace appears to be limited in the northern Lesser Antilles fore-arc whereas
355 it reaches ca 60 m asl in the southern Lesser Antilles forearc, in the Barbados Island, where the
356 highest MIS 11 shoreline angle was found between 120 and 140 m asl (Speed and Cheng, 2004). This
357 highlights the specificity of La Désirade, one of easternmost islands of the fore-arc, where can be
358 depicted vertical motions and deformations of the fore-arc since 1.5 Ma.

359 *6.3 Uplift rates at La Désirade*

360 *6.3.1. Post -Terrace 4 uplift*

361 During MIS 5e the sea level was estimated at 2 to 8 m asl (Kopp et al., 2009; Murray-Wallace and
362 Woodroffe, 2014; Rohling et al., 2014; Creveling et al., 2015) and the paleo-shoreline is presently at
363 $10 \text{ m} \pm 1$ asl. Thus, Terrace 4 experienced 2 ± 1 to 8 ± 1 m uplift since 122 ka taking into account
364 uncertainties on paleo-sea level during MIS 5e (Fig.13A). Apparent uplift rates range from 0.008 to
365 0.07 mm/y. Such rates are very low, especially for an active tectonic setting (Sieh, 1999; Henry et al.,
366 2014; Saillard et al., 2017). As the estimated paleo-shoreline angle from the top of Terrace 4 remains

367 at the same elevation around the island, the island underwent a uniform and very slow uplift after
368 MIS 5e without any significant tilting.

369 *6.3.2. Uplift between Terrace 3 and Terrace 4*

370 The paleo-shoreline angle of the MIS 9 deposits is at 36 ± 1 m asl and dates 310 ka. At this time, the
371 high sea level was estimated between 0 and 6 m asl (Rohling et al., 2014) (Fig. 13). The difference in
372 elevation between MIS 5e and MIS 9 high sea levels is 2 to 8 m. As a consequence, the MIS 9
373 paleosea level underwent 28 ± 1 to 34 ± 1 m (27m at minimum to 35m at maximum) uplift before the
374 formation of the MIS 5e coral reef at 122 ka. This uplift occurred during a time span lasting 188 ka,
375 indicative of apparent uplift rate ranging from 0.14 to 0.19 mm/y. Even if low, this rate is much
376 greater than the post MIS 5e rate. The mean uplift rate of Terrace 3 in reference to the Present-Day
377 sea level (36 ± 1 minus 0 to 6 m during 310 ka) is in the interval 0.11 to 0.14 mm/y. It is to note that
378 the Terrace 3 is scarcely preserved but found all around the island at the same elevation, thus
379 indicating the lack of tilting since 310 ka.

380 *6.3.3. Uplift between Terrace 2 and Terrace 3*

381 The shoreline angle of Terrace 2 is at 76 ± 1 m asl. During MIS 15 to 17 the high sea levels were
382 estimated to be 10 m bsl to 22 m asl (Rohling et al., 2014). The difference in elevation between
383 Terraces 2 and 3 is 40 ± 1 m. The uplift between MIS 15-17 and MIS 9 is thus in the 18 ± 1 to 50 ± 1 m
384 interval in a time range of 310 ka minimum to 390 ka maximum. The apparent uplift rate is thus
385 estimated in the 0.04–0.16 mm/y interval. The mean uplift rate of Terrace 2 in reference to the
386 Present-Day sea level ranges between 0.14 and 0.28 mm/y.

387 *6.3.4. Uplift between Terrace 1 and Terrace 2*

388 The shoreline angle of Terrace 1 is at 90 ± 1 m asl and may correspond to MIS 19 or 21 or 25 high sea
389 levels. The lowest and highest elevation of sea level for this time interval are estimated 5 m bsl and
390 19 asl, respectively (Rohling et al., 2014) (Fig. 13). The difference in elevation between terraces 1 and

391 2 is 14 ± 1 m. The extreme net values of uplift and subsidence are thus + 19 to – 7 m, respectively.
392 The time range of the uplift lasted from MIS 17 to MIS 25 at maximum (270 ka), from MIS 17 to MIS
393 19 at minimum (80 ka). We estimate that the vertical motion rate is ranging between ca 0 and + 0.24
394 mm/y. The mean uplift rate of Terrace 1 in reference to the Present-Day sea level (90 m elevation
395 minus 19 m or plus 5 m paleosea level during 80 ka minimum and 270 ka maximum) is in the interval
396 0.26 to 1.2 mm/y.

397 6.3.5. Mean uplift rate of the *A. palmata* reef platform

398 We calculate only mean uplift rate in reference to the Present-Day sea level for *the A. Palmata* reef
399 platform because of large uncertainties on its age and the age of Terrace 1. In the northeastern part
400 of the island, east of the Coulée du Grand Nord Fault and east of Le Souffleur Fault, the summit of
401 the coral platform crops out at 210 m asl at maximum (Fig. 3). In the western part of the island, the
402 platform was lowered later by the activity of main N40° and N130° trending normal faults. The
403 occurrence of large colonies of *A. palmata* in growth position is indicating a paleobathymetry of 5 m
404 at the end of deposition (Fig. 4). The minimum and maximum ages of the coral platform are those of
405 the highest sea level MIS 31 (1.07 Ma) and MIS 47 (1.48 Ma), respectively. During MIS 31 and MIS 47
406 sea level was estimated between 5 to 47 m asl (Rohling et al., 2014). The mean apparent uplift rate
407 of the coral platform in reference to the Present-Day sea level is in the range of 0.84–2.00 mm/y.

408 6.3.6. Global trend of apparent uplifts at La Désirade

409 The mean uplift rates at La Désirade, calculated in reference to the Present-Day sea level, are
410 decreasing since the *A. palmata* reef platform emergence (Fig. 13). Large uncertainties on the age of
411 the platform and the Terrace 1 do not allow precise comparison. However, the large difference in
412 uplift amplitude between the platform and Terrace 1 suggests that a severe slowing occurred after
413 the emergence of the platform. This is also suggested if only minimum uplift rate values are taken
414 into account. During the period corresponding to the terraces deposition and uplift, mean uplift rates
415 continued to decrease from 0.26-1.19 mm/y since the MIS 19-25 interval to 0.008-0.07 mm/y since

416 MIS 5e. This decrease is confirmed since Terrace 2 deposition, from 0.14-0.28 mm/y to 0.008-0.07
417 mm/y to Present-Day. Thus, La Désirade was uplifted since the *A. palmata* reef platform deposition,
418 and uplift decreased at last since 310 ka to become negligible since 122 ka but we favour a major
419 decrease in uplift rates after the platform emersion.

420 *6.4 Vertical motion and geodynamics in the Guadeloupe fore-arc since 1.5 Ma*

421 *6.4.1. Pleistocene fore-arc tectonics*

422 The Pleistocene to Present-Day fore-arc tectonics at the latitude of the Guadeloupe has been
423 described mainly as submeridian extension accommodated by E-W normal faults (Feuillet et al.,
424 2004). This extensional tectonics has been considered coeval with a local west- southwestward tilting
425 of Marie Galante Island. On La Désirade and offshore, on the Karukéra spur (SE of La Désirade), a
426 north-northeast direction of extension, oblique to the fore-arc trend, reactivates the inherited N180°
427 to N130° and N70° to N50° trending faults and is accommodated by the development of N90°
428 trending ones in the central part of the spur (Corsini et al., 2011; Lardeaux et al., 2013; Münch et al.,
429 2014; De Min et al., 2015). It is to note that the fore-arc basement, which is cropping out in La
430 Desirade only, is strongly deformed and its structure results from 140 Ma of geological evolution of
431 the Caribbean plate (Lardeaux et al., 2013). De Min et al. (2015) also showed that 1/ a differential
432 subsidence of the Karukéra spur occurred since the Oligocene, and went on during the Pleistocene, in
433 relation with the activity of the major N70° normal fault, north of La Désirade, and 2/ a major
434 eastward or trenchward tilting affected the Karukéra spur during the Pleistocene. This tilting (Fig. 15)
435 was evidenced by differential erosion of Late Pliocene/Early Pleistocene drowned coral reefs which
436 were severely eroded on the northern and western parts of the spur and preserved on the eastern
437 flank (De Min et al., 2015). This tilting is synchronous with the reactivation of N130°E-striking normal
438 faults on the spur (De Min et al., 2015). In La Désirade, we found that the *A. palmata* reef platform is
439 mainly preserved in the easternmost part of the island, i.e. in the hanging wall of La Coulée du Grand
440 Nord N130°E-striking normal fault. In the western part of this compartment, uppermost units of the

441 platform poorly crop out and the *A. Palmata* reef platform is only locally preserved in the hanging
442 walls of N40°E-striking normal faults and is eroded elsewhere. Thus, the distribution of the preserved
443 parts of the *A. palmata* reef platform is interpreted as indicative of an early Pleistocene eastward tilt
444 coeval with the one observed offshore on the Karukéra Spur and with an extensional tectonic
445 episode.

446 We evidenced that Terrace 3 and 4 on La Désirade occur at constant elevation all around the island
447 (Figs. 3, 5 and 14), indicating that the activity of the N130°E and N70°E fault systems, crosscutting the
448 island and responsible for a large offset of the *A. palmata* reef platform, occurred prior to T3
449 deposition (310 ka). As Terraces 1 and 2 were identified only in the northeastern part of the island, it
450 is difficult to say whether they were affected by fault activity. However, insofar Terraces 1 and 2
451 remain at rather constant elevation along several kilometers they do not look affected by the
452 observed brittle deformation and tilting of the *A. palmata* reef platform (Fig. 14). Moreover, the
453 mean uplift rates decreased severely after the uplift of the *A. palmata* reef platform. Thus, we
454 propose that the N70° and N130°E-striking normal fault activity and eastward tilting, coeval with the
455 uplift of the *A. palmata* reef platform, ceased mainly before Terrace 1 deposition (0.78–0.97 Ma) and
456 after the platform (1.07–1.54 Ma) deposition, *i.e.* during the Emilian–Sicilian interval.

457 The last Interglacial Maximum terrace (Terrace 4 in La Désirade) is affected by N90°E and inherited
458 N130°-striking normal faults mainly in the innermost part of the fore-arc, on Marie Galante and
459 Grande Terre, but also in the central-western part of the Karukéra spur. Onshore, this terrace is
460 lowered by recent (e.g. the Barre de l'île fault system in Marie Galante) and active (e.g. Gosier fault in
461 southern Grande Terre) faults toward the center of Marie Galante and Grippon plain grabens (Fig. 15,
462 D). However, it remains at +5 m asl in eastern and northern Grande Terre, thus indicating the lack of
463 post MIS 5 faulting and tilting in these areas.

464 At the scale of the archipelago, the organization of marine terraces is different along the coasts of
465 different islands and thus cannot result of a single regional process. We rather evidenced two major

466 deformation episodes during the last 1.5 Ma. A first one occurred after the *A. palmata* reef platform
467 and before the Terrace 1 deposition (Emilian–Sicilian interval) (Fig. 15, A and B), characterized in the
468 eastern part of the archipelago by a trenchward tilting and localized uplift in relation mainly with the
469 reactivation of N130°E inherited structures during a submeridian extensional episode. The second
470 event started since 0.78 – 0.97 Ma and is still active_ (Fig. 15 C and D), and is characterized by the
471 formation of E-W normal faults and the reactivation of N130°-striking normal faults, by differential
472 uplift of Pleistocene marine terraces and by a southwestward tilting of the Marie Galante island.

473 *6.4.2. Geodynamic implications*

474 Over the last 5 My, the 2km high oblique-to-the-trench Tiburon ridge was subducted from North to
475 South along the Lesser Antilles trench (Bangs et al., 2003; Patriat et al., 2011; Pichot et al., 2012). This
476 ridge corresponds to the western end of the North America-South America diffuse plate boundary
477 and its topography has been built in the middle-late Miocene-early Pleistocene (Patriat et al., 2011;
478 Pichot et al., 2012). During the 1.5-1 Ma interval, it was located below the northern tip of the
479 Karukéra spur, 25 km east of La Désirade (Fig. 15B). La Désirade is the easternmost emerged
480 promontory of the inner fore-arc extending southeastwards to the immersed Karukéra spur (Fig. 2)
481 that recorded a long-term regional extensional tectonics affecting the pre-structured fore-arc
482 basement and cover and reactivating structural Mesozoic inheritance (Lardeaux et al., 2013; De Min
483 et al., 2015). Along the Peru-Chile subduction zone, long-term permanent coastal uplifts coincide
484 with areas of aseismic creep on the subduction interface promoted by the subduction of ridges or
485 fracture zones (Saillard et al., 2017). Henry et al. (2014) showed that main parameter explaining
486 coastal uplift is small-scale heterogeneities of the subducting plate as aseismic ridges. The
487 magnitude and rate of coastal uplifts in fore-arcs do not appear correlated with the main
488 geodynamics parameters. Thus we interpret the coastal uplift of the fore-arc at La Désirade to be
489 related to the subduction of the Tiburon aseismic ridge. We propose that fore-arc uplift at the
490 latitude of the Guadeloupe might reflect a change in frictional properties along the subduction

491 interface persisting over a million year related to the subduction of the Tiburon ridge. In addition, it is
492 to note that subduction of aseismic ridges may also lead to fore-arc subsidence interrupted by rapid
493 uplift episodes (Clift and Vanucchi, 2004; Vannucchi et al., 2013). This is in accordance with the long-
494 term subsidence of the fore-arc at the latitude of the Guadeloupe archipelago, that is related to
495 extensional tectonics in the fore-arc and that was interrupted by at least two major uplift episodes:
496 one in late Pliocene and one in Calabrian times (Münch et al., 2014; De Min et al., 2015). The latter
497 corresponds to the emersion of the *A. palmata* reef platform between 1.48–1.07 Ma in La Désirade
498 and was also evidenced onshore and offshore throughout the archipelago (Cornée et al., 2012;
499 Münch et al., 2013, 2014; De Min et al., 2015). Since 0.78–0.97 Ma (Sicilian), uplift went on at La
500 Désirade but with low uplift rates despite its location close to the trench and the elevated slab dip
501 (60°). Indeed, these two parameters have been shown to correlate with higher uplift rates, especially
502 in accretionary convergent margins (Henry et al., 2014). Higher uplift rates were also evidenced in
503 neighboring Caribbean areas with either compressive (Barbados, Gomez et al., 2018) or transpressive
504 (western Hispaniola and Puerto Rico, Mann et al., 1995) fore-arc tectonics but these areas
505 correspond to different tectonic regime of the subduction zone, accretional frontal subduction for
506 the southern Lesser Antilles and oblique subduction in Hispaniola. The low uplift rates we evidenced
507 in La Désirade are coeval with the N-S extensional tectonics of fore-arc. Such low uplift may rather
508 correspond to erosional convergent margins (Henry et al., 2014). This is also supported by the
509 presence of both numerous trenchward dipping normal faults within the Karukéra spur and Cenozoic
510 carbonate platform sediments down the slope and close to the prism (De Min et al., 2015). Thus we
511 propose that both extensional tectonics and low uplift rates in the Guadeloupe fore-arc exemplify
512 the erosional character of the Lesser Antilles subduction zone since ~1 Ma in its central part (Bangs et
513 al., 2003; Münch et al., 2014; De Min et al., 2015) although geologic and tectonic processes included
514 accretion to form a frontal prism during former history of the central Lesser Antilles subduction zone.
515 Such varying erosional vs accretional character along subduction zones has already been shown in
516 relation with the subduction of asperities in different places (e.g. Aleutian; Von Huene et al., 2012).

517 We also evidenced a marked decrease of mean uplift rates after the emersion *A. palmata* reef
518 platform in La Désirade and a continuous decrease of uplift rates until Present-Day. The high
519 magnitude of the uplift of the platform and the higher uplift rates of the terraces were clearly coeval
520 with a Calabrian extensional tectonic episode, and both may be the surficial expression of the
521 subduction of the Tiburon ridge at the latitude of La Désirade. Bangs et al. (2003) showed that the
522 backstop was deformed by the subduction of the Tiburon ridge, allowing sediments of the
523 accretionary prism to subduct. At Present-Day the Tiburon ridge is no longer located beneath La
524 Désirade, but beneath the northern tip of the Karukéra spur *sensu lato* (Fig. 15D). This highlights that
525 the major Calabrian uplift, with high uplift rates, was related to a transient event at the subduction
526 interface provoking deep (backstop; Bangs et al., 2003) and surficial deformations. The vicinity of the
527 trench may have enhanced the strong vertical motion (Henry et al., 2014). Later, the moderate uplifts
528 cannot be directly related to this transient event and may have been controlled by various
529 parameters of the subduction zone, e.g. the high deep slab dip, the extensional tectonics of the
530 overriding plate and the erosional regime of the subduction.

531 At Present-Day the Lesser Antilles subduction zone is known to be moderately seismically active
532 compared to other subduction zones in the world, showing (i) only few earthquakes with a
533 magnitude greater than 7 along the megathrust (Ruiz et al., 2013) and (ii) most of the seismic activity
534 clusters along the active volcanic arc within the Caribbean upper plate (< 50 km depths) (Christeson
535 et al., 2003; Evain et al., 2013; Laigle et al., 2013). Moreover, at the latitude of the Guadeloupe,
536 supra-slab earthquakes with normal-faulting seismic activity above 50km depth were recorded
537 whereas deeper flat-thrust earthquakes were not observed (Laigle et al., 2013). These observations
538 may be consistent with low seismic coupling (aseismic creep) at the subduction interface. Indeed, it
539 has been proposed that the subduction of aseismic ridges provides fluids that can lubricate the
540 subduction interface in turn promoting aseismic creep along the megathrust or enhancing small
541 earthquakes occurrence (Chlieh et al., 2008; Schlaphorst et al., 2016; Saillard et al., 2017). Fluids may

542 also be responsible for high serpentinization of the supraslab mantle beneath the northern Lesser
543 Antilles arc as proposed by Gailler et al. (2017).

544

545 **7. Conclusion**

546 In La Désirade, four shorelines angles were identified between 0 and 90 asl. They are associated with
547 sediments deposited in shallow marine environment and coral reef depositional settings. The
548 deposits of the terraces rest unconformable on both the basement and the Pliocene to early
549 Pleistocene red algal and coral reef carbonate platform (Upper Plateaus) indicating a post-platform
550 deposition eastward tilt. Aragonite corals from the three lowest terraces provided U/Th ages
551 allowing to establish a new age model: Terrace 4 (+ 10 m) dates MIS 5e, Terrace 3 (+36 m) dates MIS
552 9, Terrace 2 (+ 76 m) is MIS 15 or MIS 17, Terrace 1 (+ 90 m) dates in the MIS 17 – 25 interval and the
553 coral reef platform dates in the MIS 31 - 49 interval. Integrating U/Th dating and corrections of paleo-
554 sea level and paleobathymetry of the studied platforms and terraces allow us to provide estimates of
555 the apparent uplift rate at different times since ~1.5 Ma. During Early Calabrian (1.07-1.5 to 0.78-0.96
556 Ma interval) the Upper Plateaus recorded transient deformation accommodated by NW-SE and ENE-
557 WSW trending normal fault systems. The mean uplift rate was high, in the 0.84-2.00 mm/y range.
558 Then, since late Calabrian to Present-Day, uplift rates decreased from 0.26 mm/y at least to 0.008 to
559 0.07 mm/y. This decrease is peculiarly well documented since 310 ka. The large early Calabrian uplift
560 appears to be related to the influence of the subducting, 2 km high oceanic Tiburon Ridge which
561 reached the subduction interface below the northern Karukéra Spur near 1.5 Ma ago. Later, the ridge
562 entered deeper into the mantle and its influence vanished. The decreasing uplift rates then are
563 related to other parameters of the subduction zone like the dip of the deep of the slab or the basal
564 erosion of the upper plate or the extensional reactivation of Cretaceous structures related to ancient
565 history of the basement.

566

567

568 **Acknowledgments**

569 This study was funded by the French National INSU Programs DyETI and SYSTER, the European
570 Interreg IIIB 'Caribbean Space' and FEDER (op.30-700) projects as well as by the Region Guadeloupe
571 and the French ANR GAARANTI. B. Fraisse performed the RX diffraction analysis (Réseau de Rayons X
572 et Gamma Z, Ressource technologique de l'Université de Montpellier), D. Delmas and C. Nevado are
573 thanked for thin-sections (Géosciences Montpellier). K. Pedoja (Caen University) is thanked for
574 improvement of the manuscript. P. Mann and D. Fernandez Blanco are thanked for their reviews.

575

576 **References**

577

- 578 1. Bangs, N.L., Christeson, G.L., and Shipley, T.H., 2003. Structure of the Lesser Antilles subduction
579 zone backstop and its role in a large accretionary system. *Journal of Geophysical Research*, 108,
580 2358.
- 581
- 582 2. Barnes, P.M. and Nicol, A., 2004. Formation of an active thrust triangle zone associated with
583 structural inversion in a subduction settings, eastern New Zealand. *Tectonics*, 23, TC1015.
- 584
- 585 3. Battistini, R., F. Hirschberger, C. T. Hoang, and Petit, M., 1986. La basse Terrasse corallienne
586 (Eémien) de la Guadeloupe : morphologie, datation $^{230}\text{Th}/^{234}\text{U}$, néotectonique. *Rev.*
587 *géomorph. dyn.*, XXXV, 1-10.
588 [https://www.researchgate.net/publication/291766951_The_Pleistocene_Eemian_low_coral_terr](https://www.researchgate.net/publication/291766951_The_Pleistocene_Eemian_low_coral_terrace_of_Guadeloupe_morphology_Th230U234_dating_neotectonics)
589 [ace_of_Guadeloupe_morphology_Th230U234_dating_neotectonics](https://www.researchgate.net/publication/291766951_The_Pleistocene_Eemian_low_coral_terrace_of_Guadeloupe_morphology_Th230U234_dating_neotectonics)
- 590
- 591 4. Bouysse, P., and Westercamp, D., 1990. Subduction of Atlantic aseismic ridges and Late Cenozoic
592 evolution of the Lesser Antilles island-arc. *Tectonophysics*, 175, p. 349, p. 357-355-380.

593

- 594 5. Bouysse, P., Garrabé, F., Maubussin, T. and Andreieff, P. , 1993. Carte géologique du
595 département de la Guadeloupe : Marie Galante et les îlets de Petite Terre) 1/50000, Service
596 Géologique National edn., BRGM, Orléans, France.
- 597
598 6. BRGM, 2010. Evolution et dynamique du trait de côte de l'archipel guadeloupéen. BRGM/RP-
599 58750, Final Report, Orléans (F), 93pp.
- 600
601 7. Chappell, J., 1974. Geology of Coral Terraces, Huon Peninsula, New Guinea: A Study of
602 Quaternary Tectonic Movements and Sea-Level Changes. Bulletin of the Geological Society of
603 America, 85, 553-570.
- 604
605 8. Clift, P.D., and Vannucchi, P., 2004. Controls on tectonic accretion versus erosion in subduction
606 zones: Implications for the origin and recycling of the continental crust. Reviews of Geophysics,
607 42, RG2001.
- 608
609 9. Chlieh, M., Avouac, J. P., Sieh, K., Natawidjaja, D. H., and Galetzka, J., 2008. Heterogeneous
610 coupling of the Sumatran megathrust constrained by geodetic and paleogeodetic measurements.
611 Journal of Geophysical Research: Solid Earth, 113(B5).
- 612
613 10. Christeson, G. L., Bangs, N. L., and Shipley, T. H., 2003. Deep structure of an island arc backstop,
614 Lesser Antilles subduction zone. Journal of Geophysical Research: Solid Earth, 108(B7).
- 615
616 11. Collot, J.-Y. and Fisher, M.A., 1989. Formation of fore-arc basins by collision between seamounts
617 and accretionary wedges: An example from the New Hebrides subduction zone. Geology, 17,
618 930-933.
- 619

- 620 12. Cornée, J.J., Léticée, J.L., Münch, P., Quillévé, F., Lebrun, J.F., Moissette, P., Braga, J.C., Melinte-
621 Dobrinescu, M., De Min, L., Oudet, J. and Randrianasolo, A., 2012. Sedimentology,
622 palaeoenvironments and biostratigraphy of the Pliocene-Pleistocene carbonate platform of
623 Grande- Terre (Guadeloupe, Lesser Antilles fore-arc). *Sedimentology*, 59, 1426-1451.
- 624
625 13. Corsini, M., Lardeaux, J.M., Vérati, C., Voitus, E. and Balagne, M., 2011. Discovery of Lower
626 Cretaceous synmetamorphic thrust tectonics in French Lesser Antilles (La Désirade Island,
627 Guadeloupe): Implications for Caribbean geodynamics. *Tectonics*, 30, TC4005.
- 628
629 14. Creveling, J.R., Mitrovica, J.X., Hay, C.C., Austermann, J. and Kopp, R.E., 2015. Revisiting tectonic
630 corrections applied to Pleistocene sea-level highstands. *Quaternary Science Reviews*, 111, 72-80.
- 631
632 15. DeMets, C., Jansma, P.E., Mattioli, G.S., Dixon, T.H., Farina, F., Bilham, R.G., Calais, E. and Mann,
633 P., 2000. GPS geodetic constraints on Caribbean-North America plate motion. *Geophysical*
634 *Research Letters*, 27, 437-440.
- 635
636 16. Delanghe, D., Bard, E., Hamelin, B., 2002. New TIMS constraints on the uranium-238 and
637 uranium-234 in seawaters from the main ocean basins and the Mediterranean Sea. *Marine*
638 *Chemistry*, 80, 79–93.
- 639
640 17. De Min L., Lebrun, J.F., Cornée, J.-J., Munch, P., Léticée J.-L., Quillévé, F., Melinte-Dobrinescu,
641 M., Randrianasolo A., Marcaillou, B. and Zami, F., 2015. Tectonic and sedimentary architecture of
642 the Karukéra spur: A record of the Lesser Antilles fore-arc deformations since the Neogene.
643 *Marine Geology*, 363, 15-37.
- 644

- 645 18. Deng, J. and Sykes, L.R., 1995. Determination of Euler pole for contemporary relative motion of
646 Caribbean and North American plates using slip vectors of interplate earthquakes. *Tectonics*, 14,
647 39-53.
- 648
- 649 19. de Reynal de Saint Michel, A., 1966. Carte géologique de la France et notice explicative,
650 département de la Guadeloupe, feuilles de St Martin, St Barthelemy et Tintamarre, Basse-Terre
651 et les Saintes, Marie-Galante et La Désirade, scale 1/50,000, Ministère de l'Industrie, Paris.
- 652
- 653 20. Diaz de Neira, J.A., Braga, J.C., Mediato, J., Lasseur, E., Monthel, J., Hernaiz, P.P., Pérez-Cerdan,
654 F., Lopera, E. and Thomas, A., 2015. Plio-Pleistocene paleogeography of the Llanura Costera del
655 Caribe in eastern Hispaniola (Dominican Republic): interplay of geomorphic evolution and
656 sedimentation. *Sedimentary Geology*, 325, 90-105.
- 657
- 658 21. Dixon, T.H., Farina, F., Demets, C., Jansma, P., Mann, P. and Calais, E., 1998. Relative motion
659 between the Caribbean and North American Plates and related boundary zone deformation from
660 a decade of GPS observations. *Journal of Geophysical Research*, 103, 15157-15182.
- 661
- 662 22. Dominguez, S., Lallemand, S., Malavieille, J. and von Huene, R., 1998. Upper plate deformation
663 associated with seamount subduction. *Tectonophysics*, 293, 207-224.
- 664
- 665 23. Dominguez, S., Malavieille, J. and Lallemand, S.E., 2000. Deformation of accretionary wedges in
666 response to seamount subduction: insights from sandbox experiments. *Tectonics*, 19, 182-196.
- 667
- 668 24. Evain, M., Galve, A., Charvis, P., Laigle, M., Kopp, H., Bécel, A., Weinzierl, W., Hirn, A., Flueh, E.R.,
669 Gallard, J. and the Lesser Antilles Thales scientific party, 2013. Structure of the Lesser Antilles

- 670 subduction forearc and backstop from 3D seismic refraction tomography. *Tectonophysics*, 603,
671 55-67.
- 672
- 673 25. Feuillet, N., Manighetti, I., Tapponnier, P., and Jacques, E., 2002. Arc parallel extension and
674 localization of volcanic complexes in Guadeloupe, Lesser Antilles. *Journal of Geophysical*
675 *Research: Solid Earth*, 107, ETG 3-1–ETG 3-29.
- 676
- 677 26. Feuillet, N., Tapponnier, P., Manighetti, I., Villemant, B., and King, G.C.P., 2004. Differential uplift
678 and tilt of Pleistocene reef platforms and Quaternary slip rate on the Morne-Piton normal fault
679 (Guadeloupe, French West Indies). *Journal of Geophysical Research: Solid Earth*, 109, B2.
- 680
- 681 27. Fietzke, J., Liebetrau, V., Eisenhauer, A. and Dullo, W.-C., 2005. Determination of uranium isotope
682 ratios by multi-static MIC-ICP-MS: method and implementation for precise U-and Th-series
683 isotope measurements. *Journal of Analytical Atomic Spectrometry*, 20, 395-401.
- 684
- 685 28. Gailler, L.S., Mertelet, G., Thion, I., Bouchot, V., Lebrun, J.-F. and Münch, P., 2013. Crustal
686 structure of Guadeloupe islands and the Lesser Antilles Arc from a new gravity and magnetic
687 synthesis. *Bulletin de la Société Géologique de France*, 184, 77-97.
- 688
- 689 29. Gailler, L., Arcay, D., Münch, P., Mertelet, G., Thion, I., and Lebrun, J.-F., 2017. Forearc structure
690 in the Lesser Antilles inferred from depth to the Curie temperature and thermo-mechanical
691 simulations. *Tectonophysics*, 706-707, 71-90.
- 692
- 693 30. Gomez, S., Bird, D. and Mann, P., 2018. Deep crustal structure and tectonic origin of the Tobago-
694 Barbados ridge. *Interpretation*, 6, T471-T484.
- 695

- 696 31. Gutscher, M.A., Kukowski, N., Malavieille, J. and Lallemand, S.E., 1998. Episodic imbricate
697 thrusting and underthrusting; Analog experiment and mechanical analysis applied to Alaskan
698 accretionary wedge. *Journal of Geophysical Research: Solid Earth*, 103, 10161-10176.
699
- 700 32. Henry, H., Regard, V., Pedoja, K., Husson, L., Martinod, J., Witt, C. and Heuret, A., 2014. Upper
701 Pleistocene uplifted shorelines as tracers of (local rather than global) subduction dynamics.
702 *Journal of Geodynamics* 78, 8-20.
703
- 704 33. Jara-Munoz, J., Melnick, D. and Strecker, M. R., 2015. TerraceM: A MATLAB® tool to analyze
705 marine and lacustrine terraces using high-resolution topography. *Geosphere*, 12, doi:
706 10.1130/GES01208.1.
707
- 708 34. Kopp, R. E., Simons, F. J., Mitrovica, J. X., Maloof, A. C. and Oppenheimer, M., 2009. Probabilistic
709 assessment of sea level during the last interglacial stage. *Nature* 462, 863-867.
710
- 711 35. Laigle, M., Becel, A., de Voogd, B., Sachpazi, M., Bayrakci, G., Lebrun, J.-F., and Evain, M., 2013.
712 Along-arc segmentation and interaction of subducting ridges with the Lesser Antilles subduction
713 fore-arc crust revealed by MCS imaging. *Tectonophysics*, 603, 32-54.
714
- 715 36. Lajoie, K. R., 1986. *Coastal Tectonics. Active tectonic*. N. A. Press. Washington D, C, National
716 Academic Press, 95-124.
717
- 718 37. Lallemand, S. E., 1995. High rates of arc consumption by subduction processes: some
719 consequences. *Geology*, 23, 551-554.
720

- 721 38. Lallemand, S.E., 1999. La subduction océanique. Overseas Publishers Association, Gordon and
722 Breach Science Publishers, London, 194 p.
723
- 724 39. Lardeaux, J.-M., Münch, P., Corsini, M., Cornée, J.-J., Verati, C., Lebrun, J.-F., Quillévéré, F.,
725 Melinte-Dobrinescu, M., Léticée, J.-L., Fietzke, J., Mazabraud, Y., Cordey, F. and Randrianasolo,
726 A., 2013. La Désirade island (Guadeloupe, French West Indies): a key target for deciphering the
727 role of reactivated tectonic structures in Lesser Antilles arc building. Bulletin de La Société
728 Géologique de France, 184, 21-34.
729
- 730 40. Lasserre, G., 1961. La Guadeloupe: étude géographie (Vol. 2). Union française d'Impression, 2 vol
731 Bordeaux, France, gr.in-8*, 1135 pp.
732 [https://www.abebooks.fr/servlet/BookDetailsPL?bi=5796175183&searchurl=tn%3Dla%2Bguadel](https://www.abebooks.fr/servlet/BookDetailsPL?bi=5796175183&searchurl=tn%3Dla%2Bguadeloupe%2Betude%2Bg%25E9ographie%26sortby%3D17%26an%3Dguy%2Blasserre)
733 [oupe%2Betude%2Bg%25E9ographie%26sortby%3D17%26an%3Dguy%2Blasserre](https://www.abebooks.fr/servlet/BookDetailsPL?bi=5796175183&searchurl=tn%3Dla%2Bguadeloupe%2Betude%2Bg%25E9ographie%26sortby%3D17%26an%3Dguy%2Blasserre)
734
- 735 41. Laurencin, M., Marcaillou, B., Graindorge, D., Klingelhoefer, F., Lallemand, S., Laigle, M., &
736 Lebrun, J. F., 2017. The polyphased tectonic evolution of the Anegada Passage in the northern
737 Lesser Antilles subduction zone. *Tectonics*, 36(5), 945-961.
738
- 739 42. Léticée, J. - L., 2008. Architecture d'une plateforme carbonatée insulaire plio - pleistocène en
740 domaine de marge active (avant - arc des Petites Antilles, Guadeloupe): Chronostratigraphie,
741 sédimentologie paléoenvironnements. Unpublished PhD Thesis, Pointe à Pitre, Université des
742 Antilles et de la Guyane, 261 pp. [http://www.diffusiontheses.fr/59450-these-de-leticee-jean-](http://www.diffusiontheses.fr/59450-these-de-leticee-jean-len.html)
743 [len.html](http://www.diffusiontheses.fr/59450-these-de-leticee-jean-len.html)
744
- 745 43. Lisiecki, L. E. and Raymo, M. E., 2005. A Pliocene-Pleistocene stack of 57 globally distributed
746 benthic $\delta^{18}O$ records. *Paleoceanography*, 20.1.: PA1003.

747

748 44. Mann, P., Taylor, F.W, Lawrence Edwards, R., and Teh-Lung Ku, 1995. Actively evolving
749 microplate formation by oblique collision and sideways motion along strike-slip faults: An
750 example from the northeastern Caribbean plate margin. *Tectonophysics*, 246, 1-69

751

752 45. McCann, W.R., and Sykes, L.R., 1984. Subduction of aseismic ridges beneath the Caribbean Plate:
753 Implications for the tectonics and seismic potential of the northeastern Caribbean. *Journal of*
754 *Geophysical Research: Solid Earth*, 89, 4493-4519.

755

756 46. Montaggoni, L. F. and Braithwaite, C. J., 2009. Quaternary Reefs in time and space.
757 *Developments in Marine Geology*, 5, 1-21.

758

759 47. Münch, P., Lebrun, J. - F., Cornée, J. - J., Thinon, I., Guennoc, P., Marcaillou, B., Begot, J.,
760 Bertrand, G., Bes de Berc, S., Biscarrat, K., Claud, C., De Min, L., Fournier, F., Gailler, L. - S.,
761 Graindorge, D., Léticée, J. - L., Marié, L., Mazabraud, Y., Melinte Dobrinescu, M., Moissette, P.,
762 Quillévéré, F., Verati, C. and Randrianasolo, A., 2013. Pliocene to Pleistocene carbonate systems
763 of the Guadeloupe archipelago, French Lesser Antilles: a land and sea study (the KaShallow
764 project). *Bulletin de la Société Géologique de France*, 184, 99-110.

765

766 48. Münch, P., Cornée, J.-J., Lebrun, J.-F., Quillevere, F., Verati, C., Melinte-Dobrinescu, M., Demory,
767 F., Smith, B., Jourdan, F., Lardeaux, J.-M., De Min, L., Leticée, J.-L. and Randrianasolo, A., 2014.
768 Pliocene to Pleistocene vertical movements in the fore-arc of the Lesser Antilles subduction:
769 insights from chronostratigraphy of shallow-water carbonate platforms (Guadeloupe
770 archipelago). *Journal of the Geological Society of London*, 171, 329-341.

771

- 772 49. Murray-Wallace, C. and Woodroffe, C., 2014. Quaternary sea level: a global perspective.
773 Cambridge, Cambridge University Press.
774
- 775 50. Noda, A., 2016. Forearc basins: types, geometries, and relationships to subduction zone
776 dynamics. *GSA Bulletin*, 128, 879-895.
777
- 778 51. Patriat, M., Pichot, T., Westbrook, G.K., Umber, M., Deville, E., Benard, F., Roest, W.R., Loubrieu,
779 B. and Party, A.C., 2011. Evidence for Quaternary convergence across the North America-South
780 America plate boundary zone, east of the Lesser Antilles. *Geology*, 39, 979-982.
781
- 782 52. Pedroja, K., L. Husson, V. Regard, P. R. Cobbold, E. Ostancaux, M. E. Johnson, S. Kershaw, M.
783 Saillard, J. Martinod, L. Furgerot, P. Weill and B. Delcaillau, 2011. Relative sea-level fall since the
784 last interglacial stage: Are coasts uplifting worldwide? *Earth-Science Reviews* 108, 1-15.
785
- 786 53. Pedroja, K., L. Husson, M. E. Johnson, D. Melnick, C. Witt, S. Pochat, M. Nexer, B. Delcaillau, T.
787 Pinegina, Y. Poprawski, C. Authemayou, M. Elliot, V. Regard and F. Garestier, 2014. Coastal
788 staircase sequences reflecting sea-level oscillations and tectonic uplift during the Quaternary and
789 Neogene. *Earth-Science Reviews* 132, 13-38.
790
- 791 54. Pichot, T., Patriat, M., Westbrook, G.K., Nalpas, T., Gutscher, M.A., Roest, W.R., Deville, E.,
792 Moulin, M., Aslanian, D. and Rabineau, M., 2012. The Cenozoic tectonostratigraphic evolution of
793 the Barracuda Ridge and Tiburon Rise, at the western end of the North America–South America
794 plate boundary zone. *Marine Geology*, 303–306, 154-171.
795
- 796 55. Pindell, J.L. and Kennan, L., 2009. Tectonic evolution of the Gulf of Mexico, Caribbean and
797 northern South America in the mantle reference frame: an update. In: James, K.H., Lorente, M.A.,

798 and Pindell, J.L., eds., Origin and Evolution of the Caribbean Plate. Geological Society, Special
799 Publication, 328, 1-55.
800

801 56. Pirazzoli, P. A., U. Radtke, W. S. Hantoro, C. Jouannic, C. T. Hoang, C. Causse and Best M. B., 1993.
802 A one million-year-long sequence of marine terraces on Sumba Island, Indonesia. *Marine*
803 *Geology* 109, 221-236.
804

805 57. Rohling, E.J., Foster, G.L., Grant, K.M., Marino, G., Roberts, A.P., Tamisiea, M.E. and Williams, F.,
806 2014. Sea-level and deep-sea-temperature variability over the past 5.3 million years. *Nature*, 508,
807 477-482.
808

809 58. Ruiz, M., Galve, A., Monfret, T., Sapin, M., Charvis, P., Laigle, M., Evain, M., Hirn, A., Flueh, J.,
810 Diaz, J., Lebrun J.F, and the Lesser AntillesThales scientific party, 2013. Seismic activity offshore
811 Martinique and Dominica islands (Central Lesser Antilles subduction zone) from temporary
812 onshore and offshore seismic networks. *Tectonophysics*, 603, 68-78.
813

814 59. Saillard, M., Audin, L., Rousset, B., Avouac, J. P., Chlieh, M., Hall, S. R., Husson, L. and Farber, D.
815 L., 2017. From the seismic cycle to long-term deformation: linking seismic coupling and
816 Quaternary coastal geomorphology along the Andean megathrust. *Tectonics*, 36, 241-256.
817

818 60. Saillard, M., S. R. Hall, L. Audin, D. L. Farber, G. Hérail, J. Martinod, V. Regard, R. C. Finkel and
819 Bondoux, F.,2009. Non-steady long-term uplift rates and Pleistocene marine terrace
820 development along the Andean margin of Chile (31°S) inferred from 10Be dating. *Earth and*
821 *Planetary Science Letters* 277, 50-63.
822

- 823 61. Schlaphorst, D., Kendall, J.-M., Collier, J.S., Verdon, J.P., Blundy, J., Baptie, B., Latchman, J.L.,
824 Massin, F. and Bouin, M.-P., 2016. Water, oceanic fracture zones and the lubrication of
825 subducting plate boundaries—insights from seismicity. *Geophysical Journal International*, 204,
826 1405–1420.
- 827
- 828 62. Shemenda, A.I., 1994. *Subduction. Insights from physical modeling*. London, Kluwer Academic
829 Publishers, 215 p.
- 830
- 831 63. Schellmann, G., and Radtke, U., 2004. A revised morpho-and chronostratigraphy of the Late and
832 Middle Pleistocene coral reef terraces on Southern Barbados (West Indies). *Earth-Science*
833 *Reviews*, 64, 157-187.
- 834
- 835 64. Sieh, K., Ward, S. N., Natawidjaja, D., & Suwargadi, B. W. (1999). Crustal deformation at the
836 Sumatran subduction zone revealed by coral rings. *Geophysical Research Letters*, 26(20), 3141-
837 3144.
- 838
- 839 65. Speed, R. C. and Cheng, H., 2004. Evolution of marine terraces and sea level in the last
840 interglacial, Cave Hill, Barbados. *Geological Society of America Bulletin* 116, 219-232.
- 841
- 842 66. Taylor, F. W. and Mann, P. (1991). Late Quaternary folding of coral reef terraces, Barbados.
843 *Geology*, 19, 103-106.
- 844
- 845 67. Tucker, M. E. and Wright, V. P., 1990. Diagenetic processes, products and environments. In:
846 *Carbonate sedimentology*, Blackwell Publishing Ltd, Oxford, U.K., 314-364.
847 doi: 10.1002/9781444314175.ch7
- 848

- 849 68. Vannucchi, P., Sak, P.B., Morgan, J.P., Ohkushi, K.i., Ujiie, K., Scientists, t.I.E.S., 2013. Rapid pulses
850 of uplift, subsidence, and subduction erosion offshore Central America: implications for building
851 the rock record of convergent margins. *Geology* 41, 995–998.
- 852
- 853 69. Veron, J. E. N., 2000. *Corals of the World*, vol. 1–3. Australian Institute of Marine Science,
854 Townsville, 404-405.
- 855 70. Villemant, B. and Feuillet, N., 2003. Dating open systems by the ^{238}U – ^{234}U – ^{230}Th method:
856 application to Quaternary reef terraces. *Earth and Planetary Science Letters*, 210, 105-118.
- 857
- 858 71. von Huene, R., Culotta, R., 1989. Tectonic erosion at the front of the Japan Trench convergent
859 margin. *Tectonophysics* 160, 75–90.
- 860
- 861 72. von Huene, R. and Ranero, C.R., 2003. Subduction erosion and basal friction along the sediment-
862 starved convergent margin off Antofagasta, Chile. *Journal of Geophysical Research: Solid Earth*,
863 108.B2.
- 864
- 865 73. Von Huene, R., Miller, J. J., and Weinrebe, W., 2012. Subducting plate geology in three great
866 earthquake ruptures of the western Alaska margin, Kodiak to Unimak. *Geosphere*, 8, 628-644.
- 867
- 868 74. Westercamp, D., 1980. La Désirade, carte géologique à 1: 25 000 et notice explicative. Service
869 Géologique National, Bureau de Recherches Géologiques et Minières, Orléans, France.
- 870
- 871
- 872
- 873
- 874

875 **Figures caption**

876

877 Fig. 1. Location of the studied area in the Lesser Antilles subduction zone (from Feuillet et al., 2002
878 and Münch et al., 2014).

879

880 Fig. 2. Main geological features of the Guadeloupe Archipelago, from Léticée (2008), Münch et al.
881 (2014) and De Min (2014). 1 to 7: dated Pleistocene terraces: 1, Anse Laborde (Battistini et al., 1986);
882 2, Pointe Noire (Feuillet et al., 2004); 3, Anse à l'Eau (this work) ; 4, Pointe Tarare (Feuillet et al.,
883 2004); 5, SW Désirade (Battistini et al., 1986; Feuillet et al., 2004); 6, Baie Mahault (Battistini et al.,
884 1986) ; 7, Marie Galante (Battistini et al., 1986; Feuillet et al., 2004).

885

886 Fig. 3. A: Geological map of La Désirade, from Westercamp (1980), modified from new field
887 investigations (this study); B: Lithostratigraphic succession, referred to the Grande Terre succession
888 (Cornée et al., 2012; Münch et al., 2014); C: Cross section displaying the Present-day elevations of
889 the investigated coral reef deposits.

890

891 Fig. 4. The Upper Plateaus. A: general view of the southern coast towards SW from Baie Mahault
892 area; B: general view of Pointe Adrien, northern coast; C: partially dissolved *Acropora palmata* coral
893 colonies (arrows; northeastern part of the Upper Plateaus).

894

895 Fig. 5. A: DNM with the marine terraces in the northeastern part of La Désirade; B: DNM with marine
896 terraces in southern part of La Désirade; C: topographic profiles with location of the paleoshorelines
897 surfaces; D: terminology of the different elements for the description of the terraces.

898

899 Fig. 6. Terrace 1 (loc. Fig. 3). A: field view of the 90 m asl and 76 m asl terraces surface in the Pointe
900 du Grand Abaque area; B: conglomeratic limestone with sandy calcareous matrix, red algae and
901 benthic foraminifers; pebbles are encrusted by red algae (arrows).

902

903 Fig. 7. Terrace 2 (loc. Fig. 3). A: field view of the +76 m terrace surface (arrows), Baie mahault area
904 (southern side of La Désirade); B: succession of terrace 2 at Route de La Montagne; C: field view of
905 the succession; D: cross stratification (upper arrow) and hummocky cross stratification (lower arrow)
906 in matrix supported conglomerates and microconglomeratic sandstones; E: aragonite *Diploria* coral
907 colony; F: and G microscopic views of the aragonite walls of the corals (natural light).

908

909 Fig. 8. Terrace 3 (loc. Fig. 3). A: Terraces 3 and 4 at Cul Foncé; B: lithological succession in the terrace
910 3 at Cul Foncé; C: terrace 3 at Pointe Doublé; D: horizontal wavecut surface at + 36 m, Roche du
911 large. Same legend as Fig. 7.

912

913 Fig. 9. Marine deposits of Terrace 3, Cul Foncé (loc. Fig. 3). A: conglomerates with pebbles above the
914 basement; B: 3D dunes in vertical accretion; C: parallel-bedding laminations with pebbly intervals
915 (center) and cross-trough stratification (lower arrow); D: cross-stratification; E: aragonite massive
916 coral colony DS 10-40; F: microscopic view of the coral colony (natural light). Same legend as Fig. 7.

917

918 Fig. 10. Terrace 4, Pointe Frégule (loc. Fig. 3). A: lithostratigraphic succession; B: low angle planar
919 lamination; C: basal conglomerate; D: large *Acropora palmata* colonies (arrows); E: microscopic view
920 of aragonite walls of the coral colonies (natural light). Hammer is 40 cm long. Same legend as Fig. 7.

921

922 Fig. 11. Terrace 4, Pointe Fromager, northern coast of La Désirade (loc. Fig. 3).

923

924 Fig. 12. Terrace 4 (loc. Fig. 3). A: field view at Baie Mahault beach (near cemetery); B: Dated coral at
925 Baie Mahault beach; C: microscopic view of the aragonite corals DS11-43 at Baie Mahault beach; D:
926 *Acropora palmata* boudstone (arrows); E: massive *Montastraea* colony (hammer is cm long); F:
927 terraces 3 and 4 at Pointe Mancenillier (loc. Fig. 3).

928

929 Fig. 13. Morphostratigraphy and apparent uplift rates at La Désirade. Marine isotopic stages from
930 Lisiecki and Raymo (2005) and sea level estimates from Rohling et al. (2014).

931

932 Fig. 14. Ages and elevations of the marine terraces in the Guadeloupean archipelago. Guadeloupe:
933 Battistini et al. (1986); Münch et al. (2013; 2014); Marie Galante: Feuillet et al. (2004); La Désirade:
934 this work.

935

936 Fig. 15. A: Calabrian uplifts at La Désirade; B: distribution of vertical motions and location of the
937 Tiburon Ridge below the Karukéra Spur in the Guadeloupe archipelago during Calabrian; C: Ionian to
938 Recent uplift at La Désirade; D: distribution of vertical motions and location of the Tiburon Ridge
939 below the Karukéra Spur in the Guadeloupe archipelago during Ionian to Recent. Reconstructions are
940 based on Andreïeff et al., (1989), Bouysse and Westercamp (1990), Gailler et al. (2013), De Min
941 (2014) and De Min et al. (2015).

942

943

944 **Table caption**

945

946 Table 1. Blank amounts of the isotopes used for U/Th dating.

947 Table 2. U-series results of La Désirade and Grande Terre fossil coral samples (all uncertainties

948 quoted at 95% confidence level). For the correction of detrital ^{230}Th a $^{230}\text{Th}/^{232}\text{Th}$ activity ratio of $0.6 \pm$

949 0.2 has been applied.

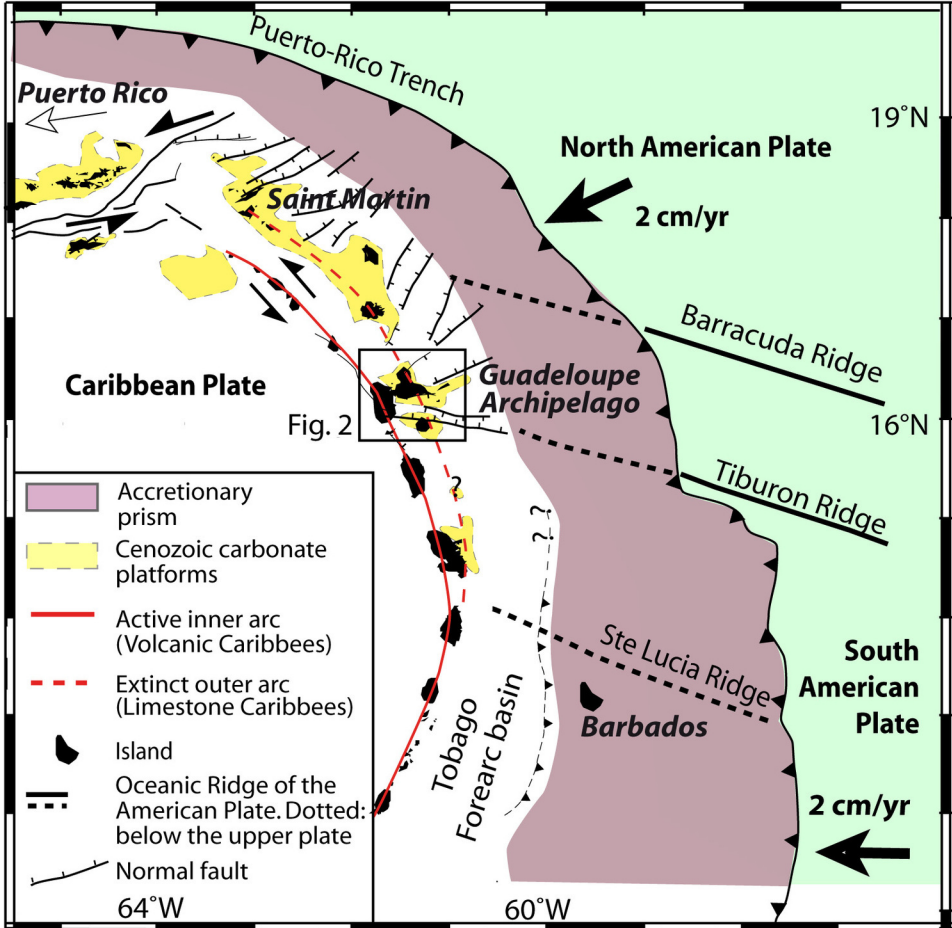
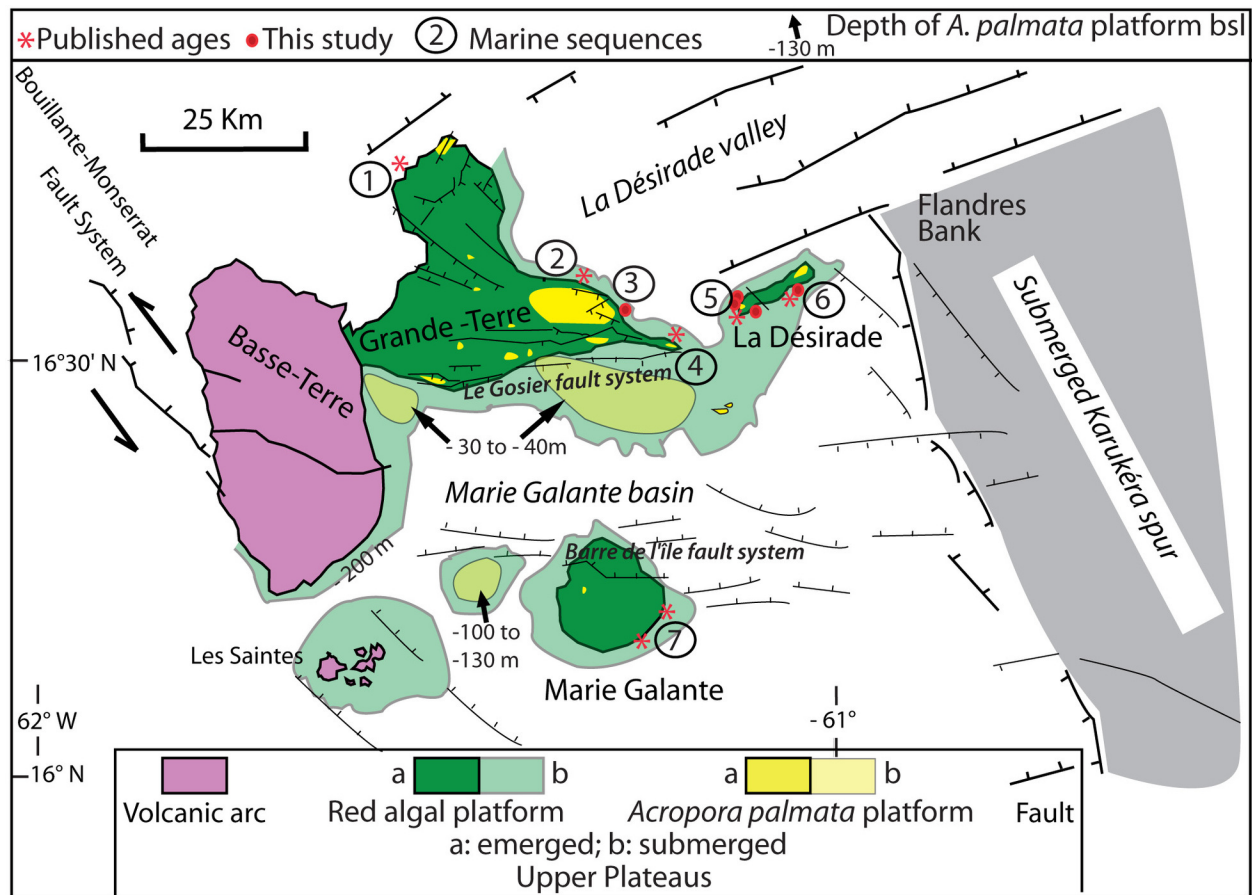
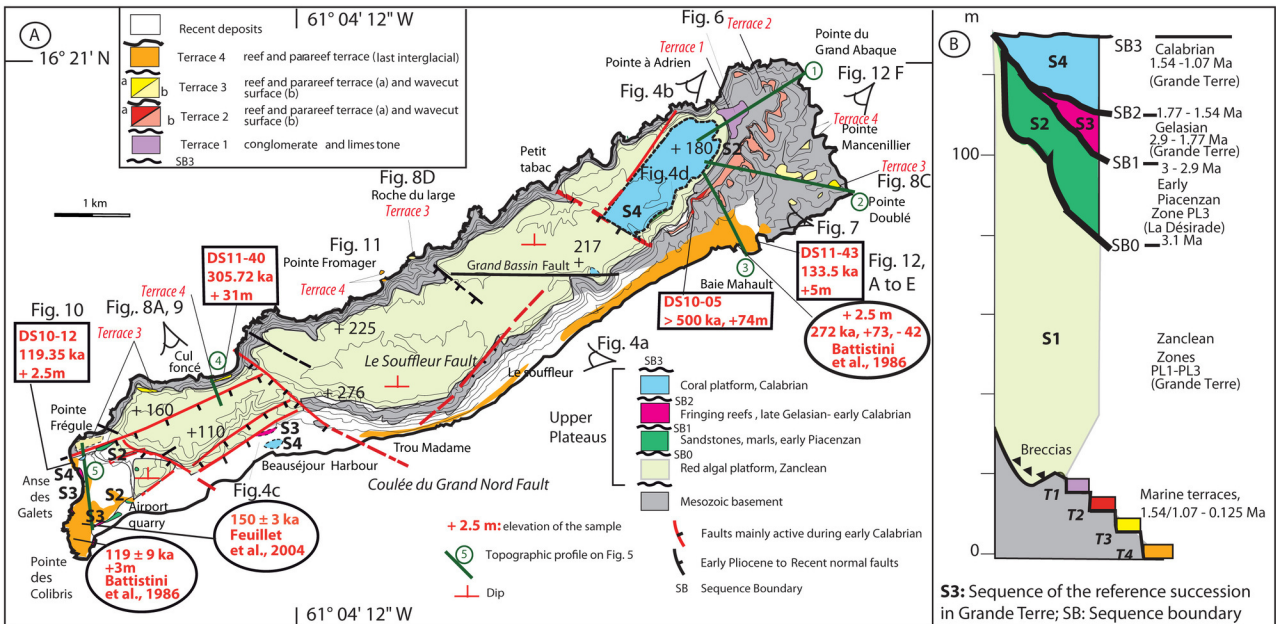


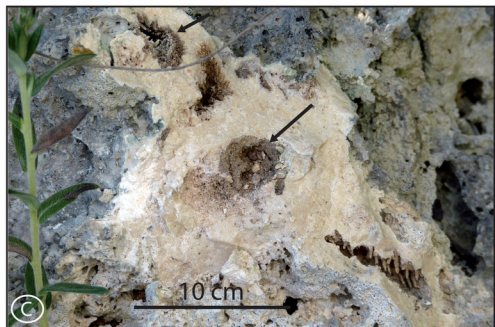
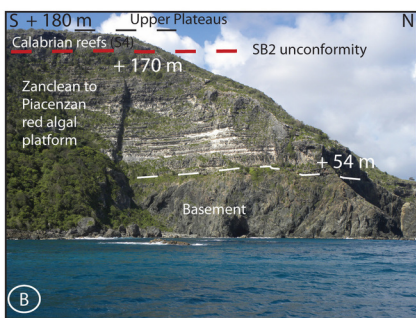
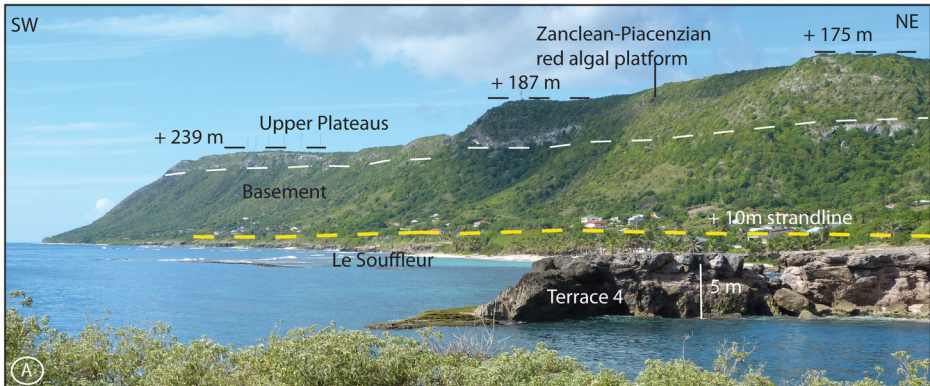
Fig. 1. Léticée et al.



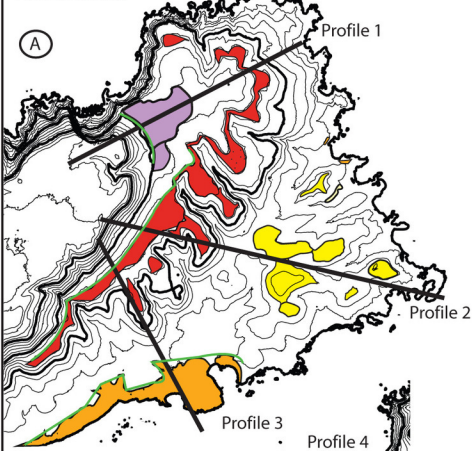
Léticée et al., Fig. 2



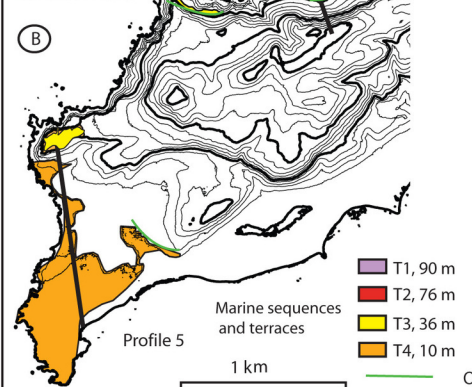
S3: Sequence of the reference succession in Grande Terre; SB: Sequence boundary



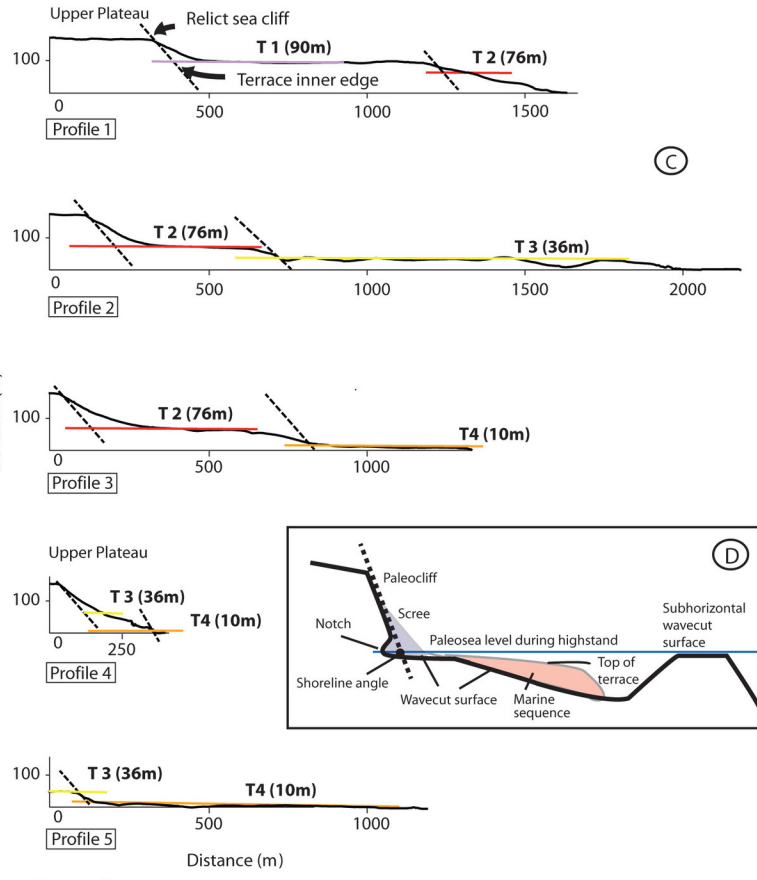
Northeast

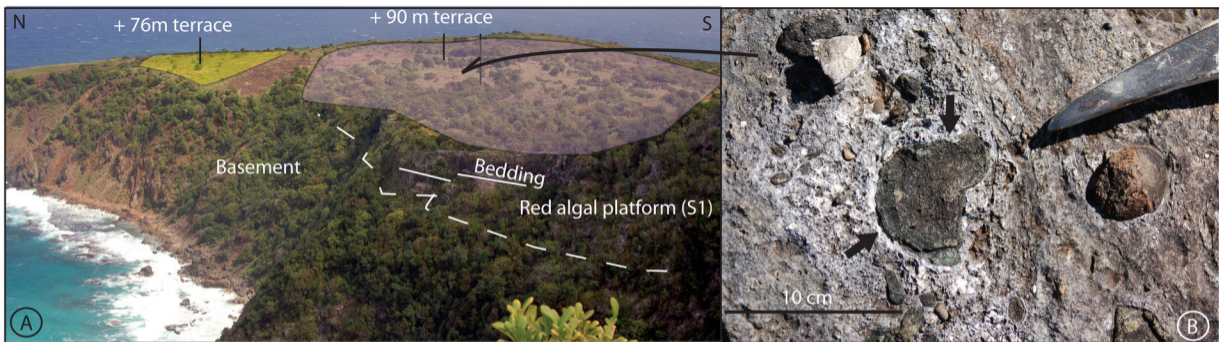


Southwest

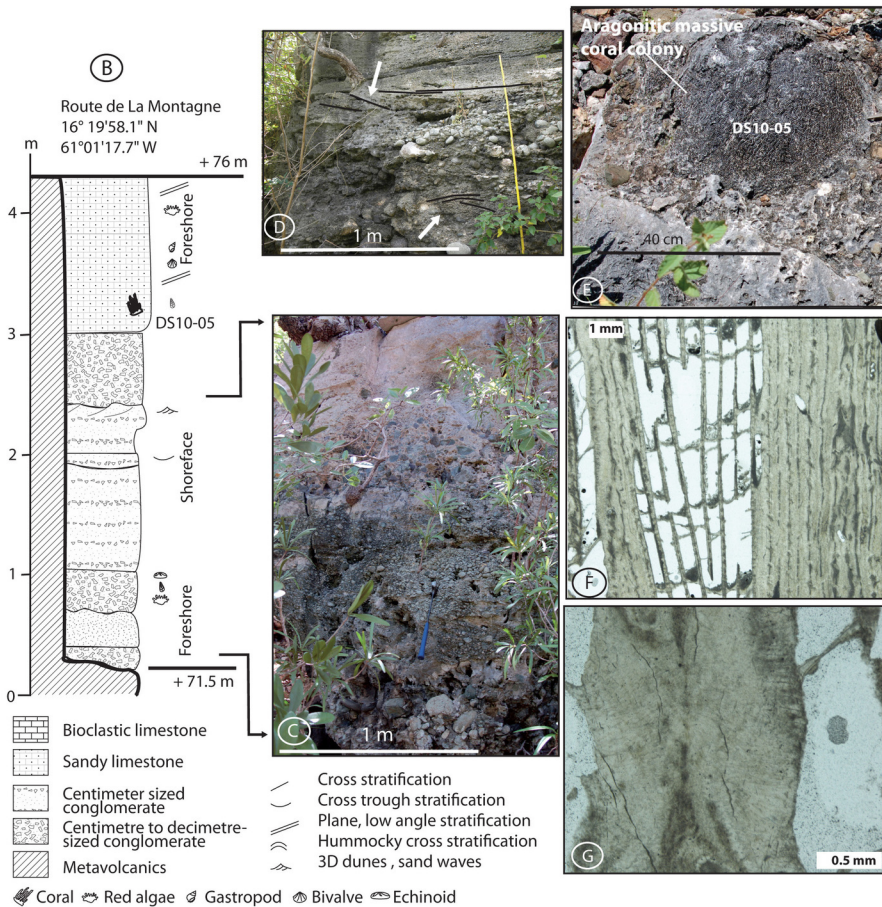
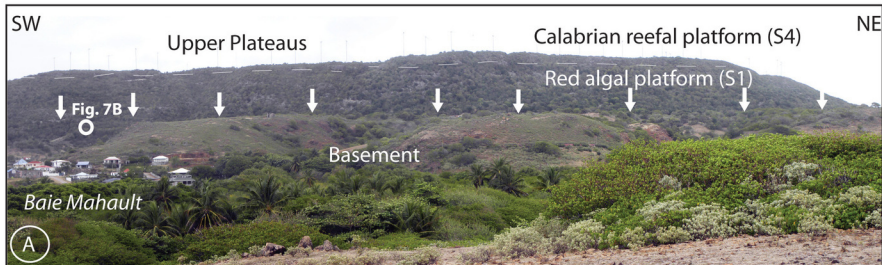


T1, 90 m
 T2, 76 m
 T3, 36 m
 T4, 10 m
 Marine sequences and terraces
 Observable shoreline

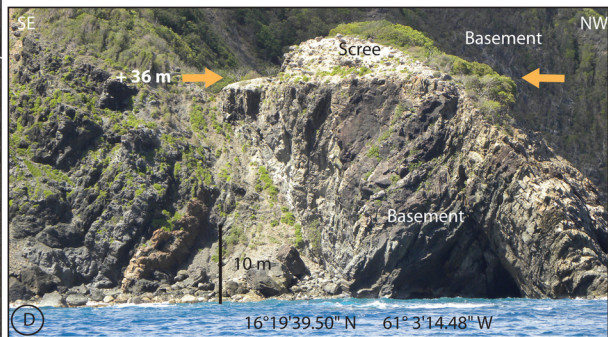
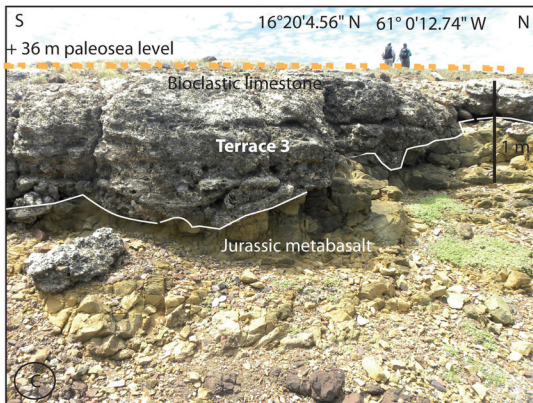
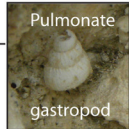
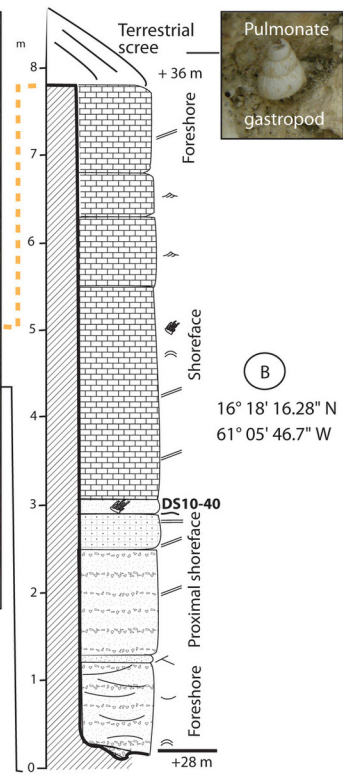
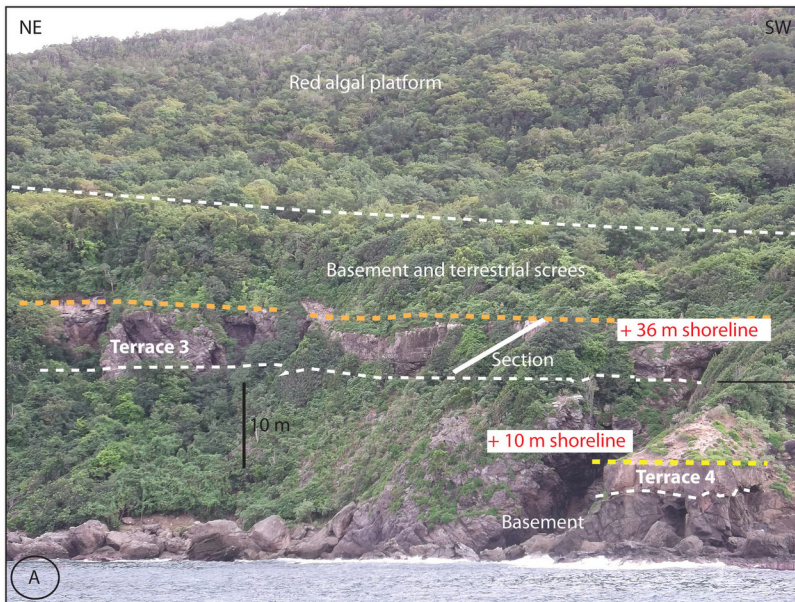


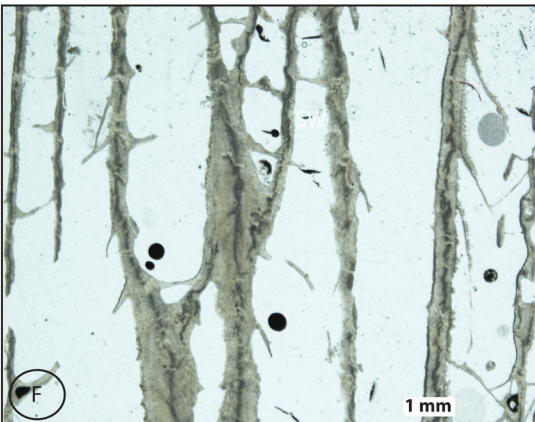
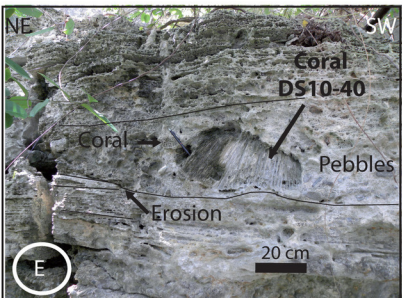
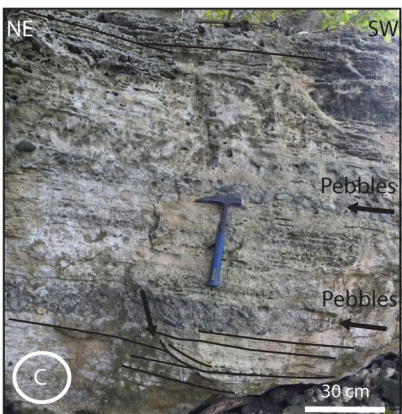
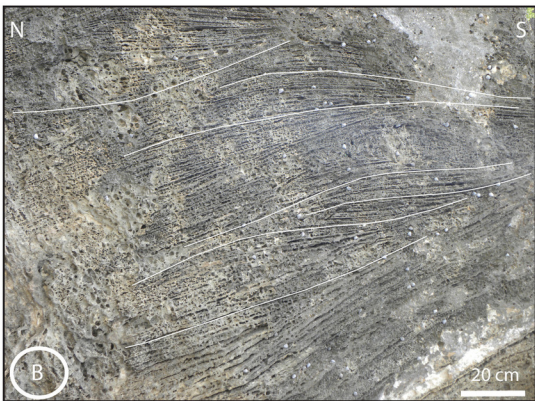
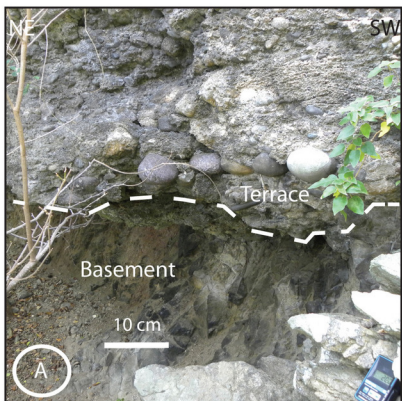


Léticée et al., fig. 6

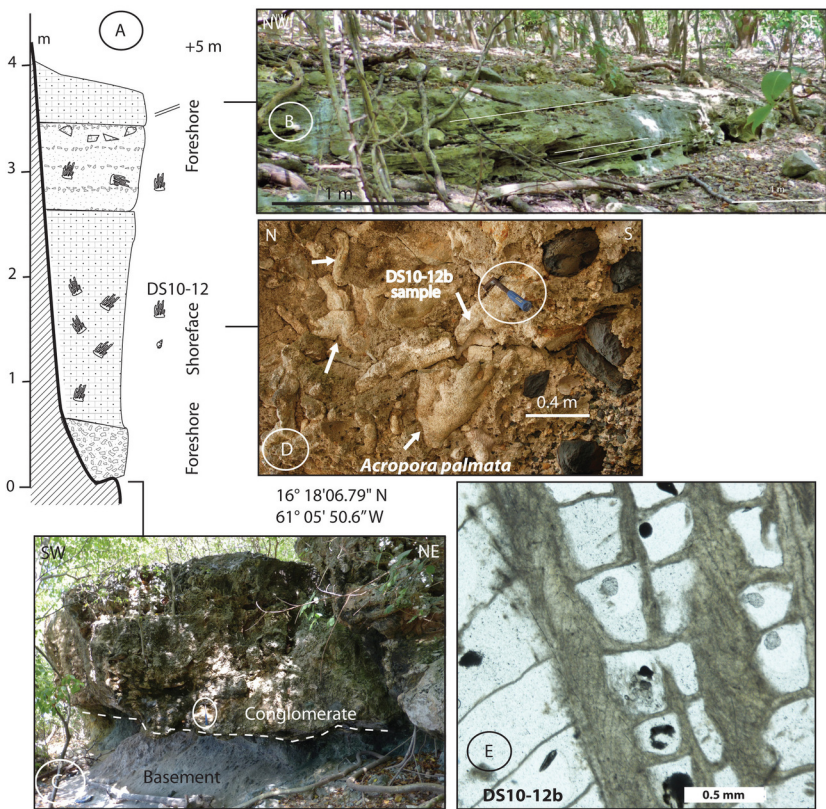


Léticée et al., Fig. 7

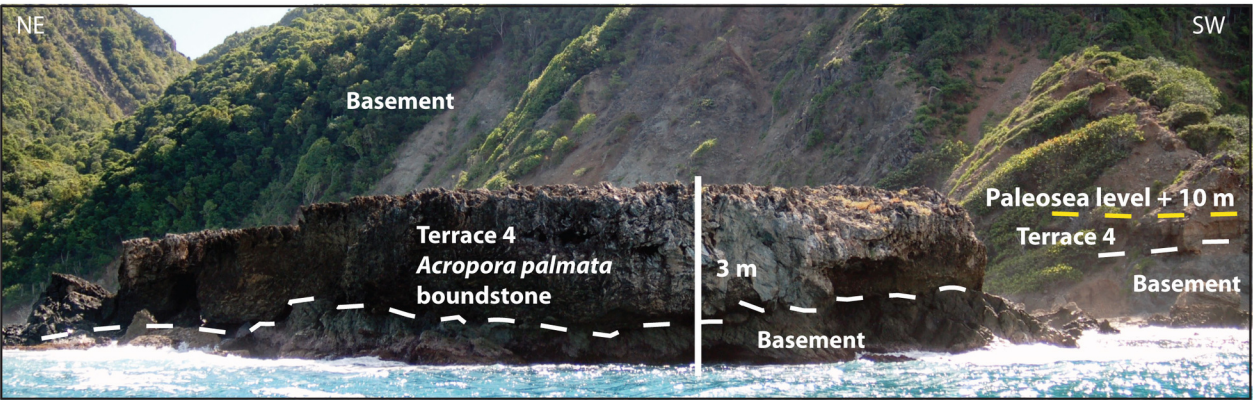




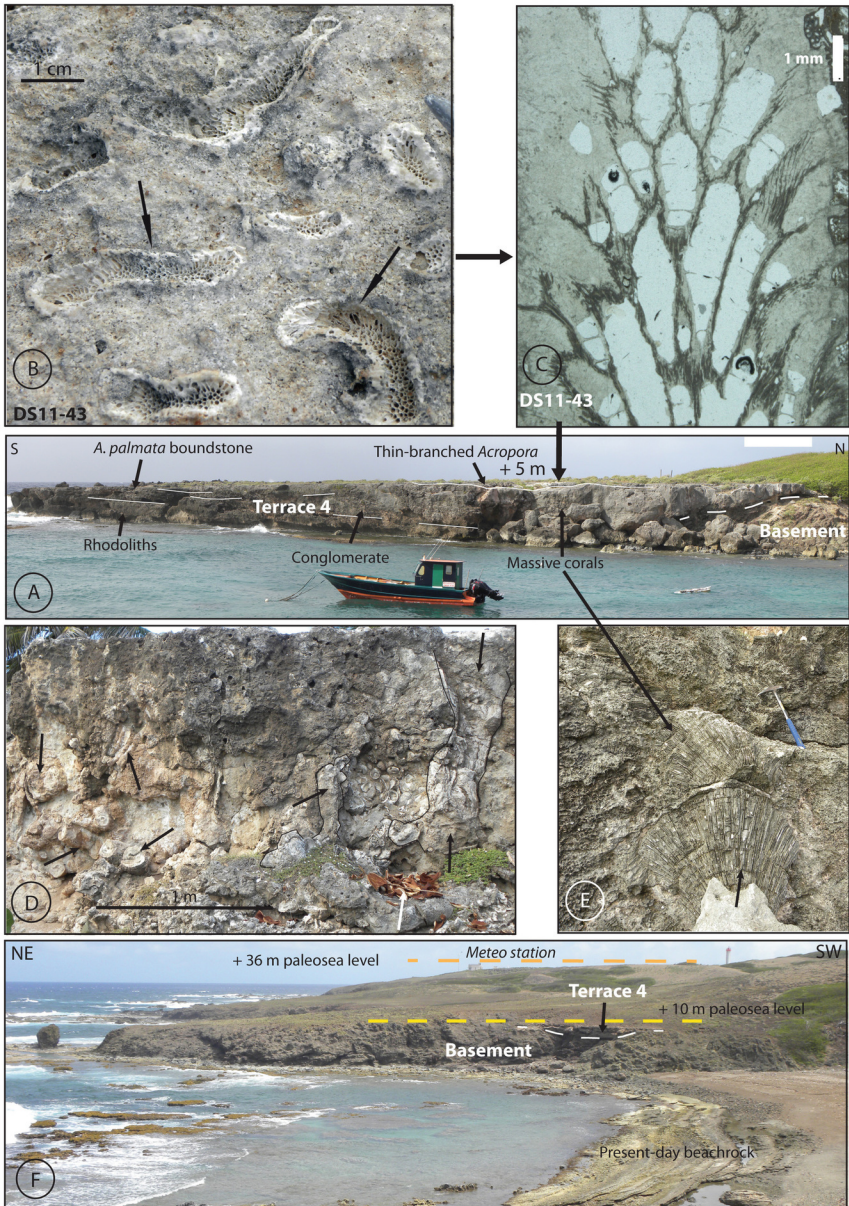
Létice et al., Fig. 9



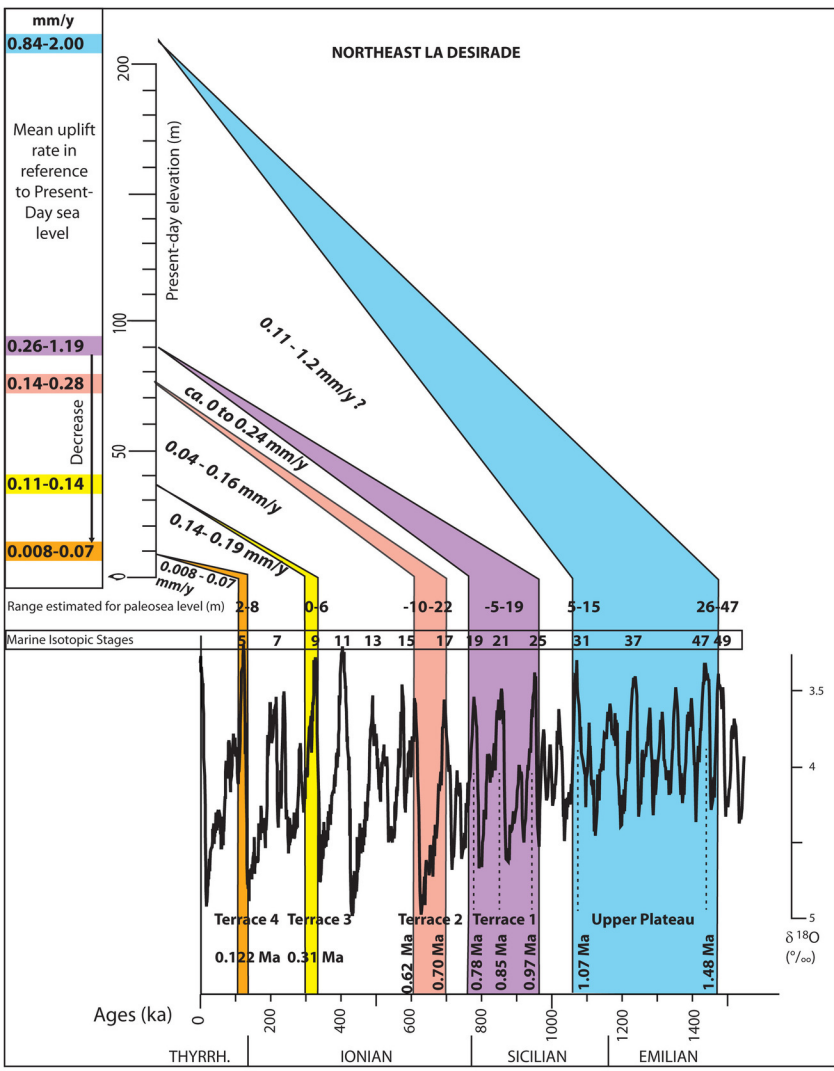
Léticée et al Fig. 10



Léticée et al., fig. 11



Léticée et al Fig. 12



Grande Terre

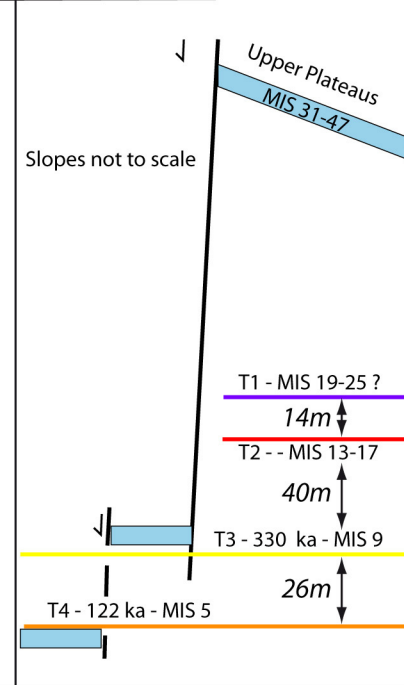
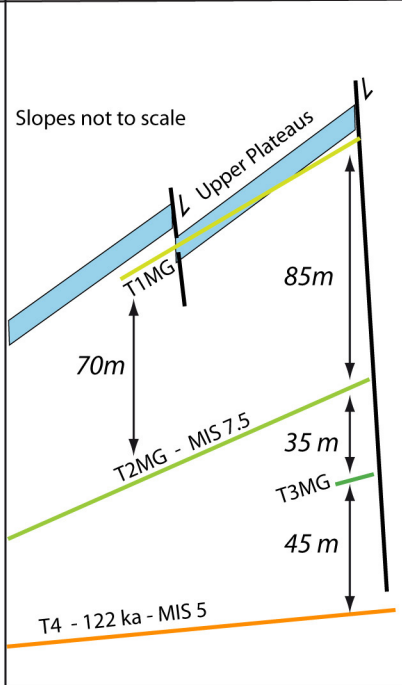
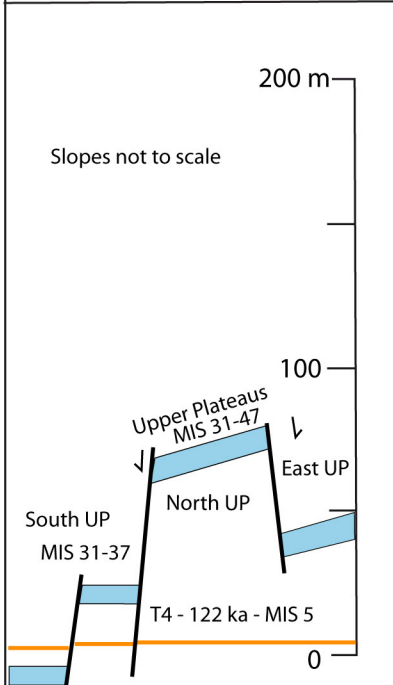
Marie-Galante

La Désirade

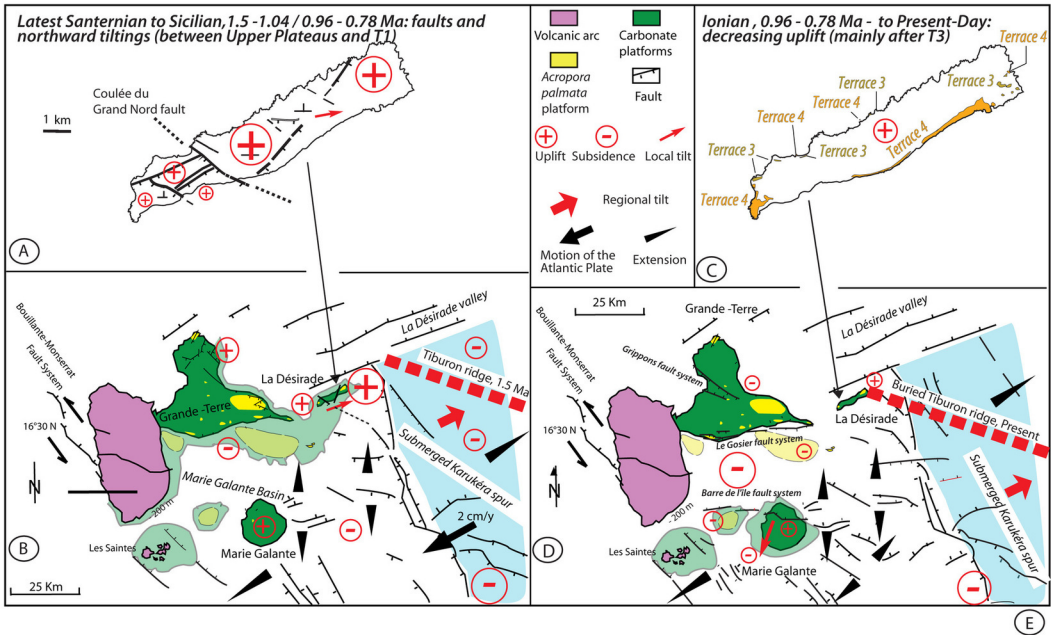
SOUTH + PETITE TERRE NORTH & EAST

SOUTH EAST & NORTH

WEST EAST



Léticée et al., fig. 14



Léticée et al., Fig. 15

Léticée et al., Table 1

isotope	blank in g
²³⁰ Th	(1.1 ± 0.6) e-16
²³² Th	(4.2 ± 2.1) e-13
²³⁴ U	(7 ± 4) e-16
²³⁸ U	(9 ± 5) e-12

Sample	Age [ka]	²³⁸ U [ppm]	²³² Th [ppb]	²³⁰ Th/ ²³⁸ U [dpm/dpm]	²³⁴ U/ ²³⁸ U [dpm/dpm]	²³⁰ Th/ ²³² Th [dpm/dpm]	Location of samples	Mineralogy
La Désirade								
DS 10-12a	126.09 ± 0.58	2.3507 ± 0.0014	0.7963 ± 0.0038	0.77708 ± 0.00085	1.1159 ± 0.0010	7100.7 ± 34.7	Terrace 4, Pointe Frégule, +2.5 m,	Aragonite 97%, Mg calcite 3%
DS 10-12b	128.19 ± 0.61	2.3035 ± 0.0013	1.0197 ± 0.0039	0.78772 ± 0.00106	1.1204 ± 0.0010	5508.2 ± 22.1	Terrace 4 Pointe Frégule, +2.5 m	Aragonite 97%, Mg calcite 3%
DS 11-43	133.50 ± 0.84	2.1278 ± 0.0018	1.6745 ± 0.0037	0.79796 ± 0.00100	1.1118 ± 0.0014	3138.6 ± 7.6	Terrace 4 Baie Mahault, + 5 m	Aragonite 96%, Calcite 4%
DS 11-40	305.72 ± 5.96	2.0724 ± 0.0015	0.6219 ± 0.0039	1.03372 ± 0.00162	1.0763 ± 0.0014	10661.8 ± 67.7	Terrace 3 Cul Foncé, + 31 m	Aragonite 97%, Mg calcite 3%
DS 10-05	>500	2.0977 ± 0.0010	0.6625 ± 0.0035	1.04099 ± 0.00125	1.0221 ± 0.0007	10202.9 ± 55.8	Terrace 2, route de La Montagne, + 74 m	Aragonite 96%, Mg calcite 4%
Grande Terre								
A-EAU 5	125.01 ± 0.44	2.3303 ± 0.0010	1.7116 ± 0.0036	0.77213 ± 0.00073	1.1141 ± 0.0007	3254.0 ± 7.3	Terrace 4 Anse à l'Eau, +5 m	Aragonite 97%, Mg calcite 3%

Léticée et al., Table 2